

# Remote Sensing of Aerosols, Clouds and Wind at Mace Head Atmospheric Research Station

Authors: Jana Preißler and Colin O'Dowd



## ENVIRONMENTAL PROTECTION AGENCY

The Environmental Protection Agency (EPA) is responsible for protecting and improving the environment as a valuable asset for the people of Ireland. We are committed to protecting people and the environment from the harmful effects of radiation and pollution.

### The work of the EPA can be divided into three main areas:

**Regulation:** *We implement effective regulation and environmental compliance systems to deliver good environmental outcomes and target those who don't comply.*

**Knowledge:** *We provide high quality, targeted and timely environmental data, information and assessment to inform decision making at all levels.*

**Advocacy:** *We work with others to advocate for a clean, productive and well protected environment and for sustainable environmental behaviour.*

## Our Responsibilities

### Licensing

We regulate the following activities so that they do not endanger human health or harm the environment:

- waste facilities (*e.g. landfills, incinerators, waste transfer stations*);
- large scale industrial activities (*e.g. pharmaceutical, cement manufacturing, power plants*);
- intensive agriculture (*e.g. pigs, poultry*);
- the contained use and controlled release of Genetically Modified Organisms (*GMOs*);
- sources of ionising radiation (*e.g. x-ray and radiotherapy equipment, industrial sources*);
- large petrol storage facilities;
- waste water discharges;
- dumping at sea activities.

### National Environmental Enforcement

- Conducting an annual programme of audits and inspections of EPA licensed facilities.
- Overseeing local authorities' environmental protection responsibilities.
- Supervising the supply of drinking water by public water suppliers.
- Working with local authorities and other agencies to tackle environmental crime by co-ordinating a national enforcement network, targeting offenders and overseeing remediation.
- Enforcing Regulations such as Waste Electrical and Electronic Equipment (WEEE), Restriction of Hazardous Substances (RoHS) and substances that deplete the ozone layer.
- Prosecuting those who flout environmental law and damage the environment.

### Water Management

- Monitoring and reporting on the quality of rivers, lakes, transitional and coastal waters of Ireland and groundwaters; measuring water levels and river flows.
- National coordination and oversight of the Water Framework Directive.
- Monitoring and reporting on Bathing Water Quality.

## Monitoring, Analysing and Reporting on the Environment

- Monitoring air quality and implementing the EU Clean Air for Europe (CAFÉ) Directive.
- Independent reporting to inform decision making by national and local government (*e.g. periodic reporting on the State of Ireland's Environment and Indicator Reports*).

## Regulating Ireland's Greenhouse Gas Emissions

- Preparing Ireland's greenhouse gas inventories and projections.
- Implementing the Emissions Trading Directive, for over 100 of the largest producers of carbon dioxide in Ireland.

## Environmental Research and Development

- Funding environmental research to identify pressures, inform policy and provide solutions in the areas of climate, water and sustainability.

## Strategic Environmental Assessment

- Assessing the impact of proposed plans and programmes on the Irish environment (*e.g. major development plans*).

## Radiological Protection

- Monitoring radiation levels, assessing exposure of people in Ireland to ionising radiation.
- Assisting in developing national plans for emergencies arising from nuclear accidents.
- Monitoring developments abroad relating to nuclear installations and radiological safety.
- Providing, or overseeing the provision of, specialist radiation protection services.

## Guidance, Accessible Information and Education

- Providing advice and guidance to industry and the public on environmental and radiological protection topics.
- Providing timely and easily accessible environmental information to encourage public participation in environmental decision-making (*e.g. My Local Environment, Radon Maps*).
- Advising Government on matters relating to radiological safety and emergency response.
- Developing a National Hazardous Waste Management Plan to prevent and manage hazardous waste.

## Awareness Raising and Behavioural Change

- Generating greater environmental awareness and influencing positive behavioural change by supporting businesses, communities and householders to become more resource efficient.
- Promoting radon testing in homes and workplaces and encouraging remediation where necessary.

## Management and structure of the EPA

The EPA is managed by a full time Board, consisting of a Director General and five Directors. The work is carried out across five Offices:

- Office of Environmental Sustainability
- Office of Environmental Enforcement
- Office of Evidence and Assessment
- Office of Radiation Protection and Environmental Monitoring
- Office of Communications and Corporate Services

The EPA is assisted by an Advisory Committee of twelve members who meet regularly to discuss issues of concern and provide advice to the Board.

**EPA RESEARCH PROGRAMME 2014–2020**

# **Remote Sensing of Aerosols, Clouds and Wind at Mace Head Atmospheric Research Station**

**(2015-CCRP-FS.24)**

## **EPA Research Report**

Prepared for the Environmental Protection Agency

by

National University of Ireland, Galway

**Authors:**

**Jana Preißler and Colin O’Dowd**

**ENVIRONMENTAL PROTECTION AGENCY**  
An Ghníomhaireacht um Chaomhnú Comhshaoil  
PO Box 3000, Johnstown Castle, Co. Wexford, Ireland

Telephone: +353 53 916 0600 Fax: +353 53 916 0699  
Email: [info@epa.ie](mailto:info@epa.ie) Website: [www.epa.ie](http://www.epa.ie)

## **ACKNOWLEDGEMENTS**

This report is published as part of the EPA Research Programme 2014–2020. The EPA Research Programme is a Government of Ireland initiative funded by the Department of Communications, Climate Action and Environment. It is administered by the Environmental Protection Agency, which has the statutory function of co-ordinating and promoting environmental research.

The Remote Sensing Division of the Mace Head Atmospheric Research Station is supported by the Irish Environmental Protection Agency (EPA), the Irish Aviation Authority (IAA) and Science Foundation Ireland (SFI). Remote sensing at Mace Head also benefits from involvement in Cloudnet; the Aerosol, Clouds and Trace gases Research Infrastructure ACTRIS and ACTRIS-2 (grant agreement numbers 262254 and 654109); the European FP7 collaborative project BACCHUS (Impact of Biogenic versus Anthropogenic emissions on Clouds and Climate: towards a Holistic UnderStanding, grant agreement number 603445); and COST action ES1303: TOPROF (Towards operational ground based profiling with ceilometers, Doppler lidars and microwave radiometers for improving weather forecasts) supported by COST (European Cooperation in Science and Technology).

The authors would like to thank John McEntagart (EPA).

## **DISCLAIMER**

Although every effort has been made to ensure the accuracy of the material contained in this publication, complete accuracy cannot be guaranteed. The Environmental Protection Agency, the authors and the steering committee members do not accept any responsibility whatsoever for loss or damage occasioned, or claimed to have been occasioned, in part or in full, as a consequence of any person acting, or refraining from acting, as a result of a matter contained in this publication. All or part of this publication may be reproduced without further permission, provided the source is acknowledged.

This report is based on research carried out/data from January 2016 to March 2019 and data collected since 2009. More recent data may have become available since the research was completed.

The EPA Research Programme addresses the need for research in Ireland to inform policymakers and other stakeholders on a range of questions in relation to environmental protection. These reports are intended as contributions to the necessary debate on the protection of the environment.

**EPA RESEARCH PROGRAMME 2014–2020**  
Published by the Environmental Protection Agency, Ireland

ISBN: 978-1-84095-907-9

July 2020

Price: Free

Online version

## Project Partners

**Jana Preißler, PhD (Research Fellow)**

Ryan Institute  
School of Physics  
National University of Ireland, Galway  
Galway  
Ireland  
Tel.: +353 (0)91 495 468  
Email: [jana.preissler@nuigalway.ie](mailto:jana.preissler@nuigalway.ie)

**Professor Colin O'Dowd (Project Coordinator)**

Ryan Institute  
School of Physics  
National University of Ireland, Galway  
Galway  
Ireland  
Tel.: +353 (0)87 811 4988  
Email: [colin.odowd@nuigalway.ie](mailto:colin.odowd@nuigalway.ie)



# Contents

|  |            |
|--|------------|
| <b>Acknowledgements</b>                                  | <b>ii</b>  |
| <b>Disclaimer</b>  | <b>ii</b>  |
| <b>Project Partners</b>                                  | <b>iii</b> |
| <b>List of Figures</b>                                   | <b>vi</b>  |
| <b>List of Tables</b>                                    | <b>vii</b> |
| <b>Executive Summary</b>                                 | <b>ix</b>  |
| <b>1 Introduction</b>                                    | <b>1</b>   |
| 1.1 Remote Sensing at Mace Head                          | 1          |
| 1.2 Objectives of This Fellowship                        | 2          |
| 1.3 Structure of This Report                             | 4          |
| <b>2 Aerosol Profiling</b>                               | <b>5</b>   |
| 2.1 Ceilometer Calibration                               | 5          |
| 2.2 Aerosol Layer Detection                              | 5          |
| 2.3 Aerosol Quantification                               | 6          |
| 2.4 Case Studies of Extreme Pollution                    | 8          |
| 2.5 Copernicus Atmosphere Monitoring Service Validation  | 10         |
| <b>3 Cloud Profiling</b>                                 | <b>12</b>  |
| 3.1 Cloud Properties                                     | 12         |
| 3.2 Cloud Parcel Model                                   | 14         |
| 3.3 Ground- and Satellite-based Remote Sensing of Clouds | 14         |
| <b>4 Wind Profiling</b>                                  | <b>16</b>  |
| 4.1 Wind Lidar Data Processing                           | 16         |
| 4.2 Wind Characteristics at Mace Head                    | 19         |
| <b>5 Summary and Recommendations</b>                     | <b>22</b>  |
| 5.1 Conclusions  | 23         |
| 5.2 Recommendations                                      | 23         |
| <b>References</b>  | <b>25</b>  |
| <b>Abbreviations</b>                                     | <b>28</b>  |

## List of Figures

|             |   |    |
|-------------|---|----|
| Figure 2.1. | Feature mask combining information from cloud radar – clouds, rain and non-spherical large aerosol particles – and ceilometer profiles for an example case on 10 May 2016   | 6  |
| Figure 2.2. | Uncalibrated ceilometer backscatter signal, ABL top and RL top for the same example case as in Figure 2.1   | 7  |
| Figure 2.3. | (a) Time–height display of backscatter coefficient profiles from the ceilometer and (b) aerosol mass concentration profiles over Mace Head, on 26 June 2013   | 7  |
| Figure 2.4. | Ceilometer signal, mass concentration of absorbing aerosol, feature mask for four episodes of extreme air pollution at ground level, or high aerosol load in the free troposphere, of different aerosol types and from different sources. (a) Volcanic aerosol from Eyjafjallajökull, Iceland; (b) mineral dust from the Sahara; (c) wildfire smoke from North America; (d) anthropogenic pollution from Europe | 9  |
| Figure 2.5. | Observation-background statistics comparing CAMS forecasts with ceilometer measurements for August 2019 from the monthly E-Profile report   | 10 |
| Figure 3.1. | Vertical profiles of LWC, $r_{\text{eff}}$ and CDNC derived from LOAC, BASTA and initial and improved SYRSOC versions   | 13 |
| Figure 3.2. | Comparison of CTH from satellite-based SEVIRI and ground-based cloud radar at Mace Head on (a) 11 June 2017 and (b) 12 June 2017  | 15 |
| Figure 4.1. | Flow chart of the WindCube Doppler lidar output and all products generated by the Python-based WindCube software package  | 17 |
| Figure 4.2. | Schematic illustration of the VAD scan pattern with 12 beams and sine fit procedure to obtain horizontal wind speed and direction   | 18 |
| Figure 4.3. | (a) Monthly distributions of horizontal wind speed and (b) distribution of horizontal wind direction from Doppler wind lidar at the lowest range bin at 39 m agl from 2 years of observations   | 20 |
| Figure 4.4. | LLJ (a) number, (b) peak altitude, (c) peak wind speed and (d) peak wind direction from 2 years of Doppler wind lidar observations  | 21 |



## List of Tables

|            |   |    |
|------------|---|----|
| Table 2.1. | Volume and mass concentrations from ground-based in situ measurements and normalised layer IBS from ceilometer measurements for four case studies               | 10 |
| Table 3.1. | Comparison of measured and modelled CDNC and supersaturation from the Fortran model for CP and MP air masses  | 14 |
| Table 4.1. | Data availability depending on CNR thresholds, tested on full profiles of VAD scans at a 15° elevation angle, over 24 hours on the example day 26 February 2018 | 18 |



# Executive Summary

The power of remote sensing lies in its ability to automatically and continuously characterise parts of the atmosphere that can be far away from the sensor, e.g. at high altitudes from the ground in the case of this study. In addition, its methods are non-intrusive, leaving the studied medium as it is, without altering its properties. Thus, remote sensing offers information that cannot be provided by ground-based *in situ* measurements. This fellowship focused on continuous high-resolution (vertical and temporal) profiling of the atmosphere over Mace Head Atmospheric Research Station using active and passive ground-based remote sensing techniques. A cloud radar, ceilometer, microwave radiometer and wind lidar were used to obtain profiles of cloud properties, aerosol concentration, temperature, humidity and wind characteristics (speed, direction, shear, turbulence). In addition, the expansive database of past measurements was exploited to study cases of extreme air pollution, to better understand cloud processes and to investigate coastal wind profiles.

To understand pollution levels measured near the Earth's surface, a supplementary observation of air pollution at higher altitudes is necessary. In this fellowship it was essential to find out where extreme air pollution came from (local pollution and transboundary air pollution) and how long the extreme pollution event persisted aloft, altering the amount of incoming solar radiation.

Routine *in situ* observations of clouds are rare and commonly available only in fog or at high-altitude stations. Therefore, cloud remote sensing is necessary and was used in this fellowship to study the cloud base and cloud top height, the cloud's radiative properties (optical thickness, cloud top albedo), and cloud formation and lifetime, and to validate cloud models.

Wind is a common standard variable recorded at a dense network of meteorological stations worldwide. Generally, it is measured at 10 m above ground by

meteorological services and fed into global forecast models. Wind profiles from remote sensing have the additional value of analysing large-scale flow patterns, unaffected by local orographic features, and of providing vertical wind shear and turbulence, essential for aircraft safety and the wind energy sector, as demonstrated in a study of 2-year wind characteristics at Mace Head.

In addition to contributing to high-impact research studies in past years, remote sensing data were also sent to the European-scale networks Cloudnet and E-Profile for joint processing and large-scale studies. The existence of such networks underlines the importance of ground-based remote sensing of the atmosphere at a continental scale. Remote sensing at Mace Head provides a large part of the Irish contribution to those pan-European networks.

For a comprehensive view of the atmosphere over the Irish west coast and subsequently a better understanding and forecast of atmospheric processes like storms, extreme pollution events and the effects of climate change, remote sensing at Mace Head will be invaluable. Continuous operation is crucial to study the complexity of coastal atmospheric processes and automatic processing is necessary to handle large numbers of data and distil essential information from the data.

Based on these considerations, continuation of Irish remote sensing is highly recommended, ideally as a supplement to existing *in situ* instrumentation (standard meteorology, aerosol characterisation, trace gas measurements). The Met Éireann station Valentia in County Kerry operates a ceilometer, a microwave radiometer and a wind lidar and is a good example of remote sensing efforts in addition to those at Mace Head Atmospheric Research Station. To extend coverage over Ireland, more remote sensing nodes should be established, preferably at existing atmospheric observatories.



# 1 Introduction

Remote sensing is based on measuring and characterising objects by interacting with them indirectly using some form of radiation. In atmospheric research, this has powerful implications, as the studied mediums – mostly aerosols, cloud particles and molecules – are not disturbed or do not have their properties altered by the measurement procedure itself, which is often the case for *in situ* observations, where a portion of air is sampled, i.e. trapped, sometimes modified (dried, compressed, etc.) and studied. In addition, using remote sensing, the studied medium can be far from the sensor itself, which makes it an ideal tool to investigate all levels of the atmosphere without the need for balloons, aircraft or other vehicles, which are comparably complicated and expensive to deploy. Remote sensing can be separated into active remote sensing, where the sensor emits radiation and receives a fraction of that radiation returned by the object of interest, and passive remote sensing, where the sensor detects naturally occurring radiation that interacted with the object of interest. In the atmosphere, these naturally occurring radiation sources can be sunlight (ultraviolet, visible and infrared radiation), terrestrial infrared radiation or microwave radiation. Using different kinds of remote sensing instruments, a large variety of atmospheric components can be studied, e.g. profiles of aerosols, clouds, temperature, humidity, horizontal wind speed and direction, vertical wind, concentration of trace gases, and water vapour. In section 1.1, the capabilities of remote sensing at the Mace Head Atmospheric Research Station in Carna, County Galway, are outlined. This report focuses on ground-based remote sensing, although a few satellite-based remote sensing applications were studied as well.

Generally, a number of remote sensing products are of high importance to society, as they link directly to air quality and health (profiles of aerosol concentration, emission monitoring, detection of transboundary air pollution) and renewable energy – and hence sustainability – as well as aviation safety (profiles of wind speed, wind shear and turbulence), environmental policies (constraining modelled emissions) and understanding of climate change (aerosol–cloud interaction, long-term monitoring).

In the European context, “Copernicus is the European Union’s Earth Observation Programme, looking at our planet and its environment for the ultimate benefit of all European citizens” (EC, 2015). The Copernicus Atmosphere Monitoring Service (CAMS) provides consistent and quality-controlled information related to air pollution and health, solar energy, greenhouse gases and climate forcing, everywhere in the world, and it is implemented by the European Centre for Medium-Range Weather Forecasts. Although CAMS includes ground-based observations for integration and validation, further remote sensing sites can act as independent validation points for Copernicus and CAMS products.

In the Irish context, aerosol detection and quantification and air quality monitoring in rural and urban environments from ground and satellite remote sensing are desirable, including monitoring of localised events, such as uncontrolled wildfires or extreme urban pollution. In addition, observation and quantification of transboundary intrusion of air pollution is possible using existing remote sensors, for example smoke from large wildfires in North America or Siberia, Saharan dust or volcanic eruptions. Ground-based remote sensing in Ireland is limited to the two national World Meteorological Organization (WMO) Global Atmosphere Watch (GAW) sites – Valentia, operated by Met Éireann, and Mace Head, operated by National University of Ireland, Galway (NUIG) – and one single lidar, which is operated infrequently by University College Cork and which is included in the European Aerosol Research Lidar Network (EARLINET).

## 1.1 Remote Sensing at Mace Head

Mace Head is situated on the Irish west coast (53.33° N, 9.90° W), with the remote sensing instruments being located about 21 m above sea level and about 300 m from the shoreline. Remote sensors used in this work include passive and active sensors, which are all located at Mace Head. Emitting laser radiation of a near-infrared wavelength (1064 nm) and pointing towards the zenith, the ceilometer is an active remote sensor that was originally designed to detect cloud base altitude as the strongest peak in the

backscattered signal. Using the time lag between the sent and received signals of a pulsed laser, the altitude can be calculated (ranging). Some ceilometers, including the CHM15k model from Jenoptik/Lufft (Germany), have lasers that are powerful enough to detect the strong peak caused by backscatter not only from cloud droplets at the cloud base but also from aerosol particles that the laser pulse encounters on the way, which makes the ceilometers useful tools for aerosol profiling and quantification.

The cloud radar at Mace Head emits and receives microwave radiation with a frequency of 35.5 GHz and uses the ranging capability for profiling of cloud droplets, ice crystals and rain. The third active sensor used in this work is a scanning Doppler wind lidar emitting and receiving at 1543 nm. In addition to profiling aerosols and clouds, it records spectra of the returned radiation and from this information can infer the speed at which the detected particles move. Combining this capability with certain scan patterns, profiles of horizontal wind speed and direction can be calculated.

The microwave radiometer is a passive sensor that detects microwave radiation in 14 detection channels from different layers of the atmosphere to infer profiles of temperature and humidity. It makes use of steep slopes in the absorption spectrum near the oxygen absorption lines (for temperature detection; seven channels between 51 and 59 GHz) and near the water vapour absorption line (for humidity measurement; six channels between 22 and 28 GHz). The remaining channel, at 31.4 GHz, is used to calculate the column of liquid water content (LWC), also called the liquid water path (LWP).

In the past, the following remote sensing studies using instruments located at Mace Head were performed. Martucci *et al.* (2010) demonstrated the ability of ceilometers to detect not only the cloud base but also the top of the atmospheric boundary layer (ABL). The boundary layer depth is an important parameter, as air quality and aerosol concentrations are strongly linked to processes in the boundary layer, as previously highlighted by Li *et al.* (2017) and Lin *et al.* (2018). Severe pollution can even cause a

positive feedback loop on the boundary layer depth (Tie *et al.*, 2017).

To study aerosol–cloud interaction and its implication for climate change, Martucci and O'Dowd (2011) introduced an algorithm to combine measurements from a set of remote sensing instruments to calculate microphysical cloud properties, namely the number of cloud droplets in a volume, the radius of these cloud droplets, the LWC of the clouds, cloud optical thickness (COT) and cloud albedo. This algorithm, Synergistic Remote Sensing of Clouds (SYRSOC), was then used by Preißler *et al.* (2016) to investigate the relationship between aerosols of different types from different geographical sources and the abovementioned cloud properties using a set of ground-based remote sensing instruments located at Mace Head. The authors found larger cloud droplet number concentrations (CDNCs) and smaller effective cloud droplet radii in more polluted conditions. COT and cloud albedo were lower in cleaner air masses and higher in more polluted conditions. This implies that clouds in polluted air reflect more sunlight back into space than clouds in clean air and that clouds in polluted air counter a warming of the Earth's surface, as proposed by previous research (Twomey, 1977; Lohmann and Feichter, 2005).

Real-time data streams from satellite remote sensing were set up at NUIG to complement the extensive ground-based remote sensing suite and form the data system StreamAIR-RS, eventually feeding into the StreamAIR system of NUIG.<sup>1</sup> Satellite observations include aerosol backscatter data from the satellite-borne lidar CALIOP (Cloud-Aerosol Lidar with Orthogonal Polarization), sea surface wind speed and direction from synthetic aperture radar on Copernicus satellites Sentinel 1A and 1B, and cloud top properties from MODIS (Moderate Resolution Imaging Spectroradiometer) and SEVIRI (Spinning Enhanced Visible and Infrared Imager).

## **1.2 Objectives of This Fellowship**

In this fellowship, the remote sensing capabilities at Mace Head were combined to meet the six originally proposed targets listed in sections 1.2.1–1.2.6.

---

<sup>1</sup> <http://streamair.nuigalway.ie/> (accessed August 2019).

### ***1.2.1 Added value from the combination of remote sensing instruments at Mace Head***

Each instrument on its own delivers important data in a high temporal and vertical resolution (from 1 s to 1 min and from 10 to 75 m, respectively). However, the combination of the instruments' products can add considerably to their value. One example is the identification and distinction of aerosol and cloud layers by combining ceilometer with cloud radar profiles. Because of its near-infrared laser emission, the ceilometer provides profiles of aerosol layers. It is, however, limited in capturing in-cloud profiles, because the laser radiation is attenuated shortly after it enters the cloud. Radar profiles, on the other hand, are available for the full extent of the cloud, but are very limited for aerosol detection. With a combined aerosol–cloud mask we gain a more comprehensive view of the atmospheric composition over Mace Head.

Such a mask can then be used to determine the boundary layer depth in order to study local air pollution or to track layers of high aerosol load above the boundary layer, which can be clear indicators of transboundary air pollution.

### ***1.2.2 Continue providing near real-time observations of atmospheric profiles***

Running a large suite of sophisticated remote sensing instruments requires constant monitoring, regular quality control and occasional maintenance or repair. The remote sensing database of Mace Head includes more than 10 years of nearly continuous high-quality profiles of aerosols, clouds, temperature and humidity.

Such a long-term database is invaluable to characterise the seasonality of aerosol load and cloud properties, as well as to establish a climatology of these parameters.

### ***1.2.3 Improve existing procedures and add new products***

Although all remote sensing instruments at Mace Head are running unattended and continuously, and automatic raw data transfer to NUIG is in place, detailed analysis used to be mostly done on a

case study basis. As part of this target, the ability to combine different measurements was much improved by the implementation of automatic retrieval procedures for the vast numbers of data available.

For example, aerosol quantification is subject to large uncertainties but can be improved by using properly calibrated ceilometer data for a more robust calculation of aerosol load along the vertical profile. Furthermore, the determination of cloud properties and the study of aerosol–cloud interaction were only done for selected cases. The algorithm for calculating microphysical cloud properties is limited to very particular conditions; these, however, can be determined using cloud radar data. Using thresholds to find suitable cloud periods for an automatic daily run of the algorithm was part of this target.

Compared with the other instruments, the wind lidar is relatively new, with data available since 2017. The instrument automatically delivers radial wind, carrier-to-noise ratio (CNR) and attenuated backscatter. In this target, those data were converted into profiles of horizontal wind speed and direction, vertical wind, wind shear and turbulence.

### ***1.2.4 In-depth study of the existing database of remote sensing observations***

Most of the remote sensing instruments at Mace Head have been running 24/7 for a number of years. This operating mode has accumulated a very large set of data with a huge potential in underpinning findings from carefully selected and analysed case studies with statistically significant results. It was proposed to use the archived data for a characterisation of aerosol from different sources in terms of backscatter and extinction profiles, as well as mass concentration using ceilometer and, for recent cases, wind lidar data.

This part of the target was changed to develop a cloud parcel model for a detailed investigation of aerosol–cloud interaction, making use of ground-based *in situ* aerosol measurements to model profiles, and comparison with measured cloud profiles from remote sensing. In addition, a 2-year study of wind characteristics at Mace Head was performed, looking at the seasonality of wind speed and direction, as well as the occurrence of low-level jets (LLJs), which

introduce high wind shear and turbulence at altitudes relevant to on- and off-shore wind turbines, hence affecting wind energy production.

### ***1.2.5 Continue participation in international projects and collaborations***

The remote sensing division of Mace Head plays an active role in the following projects:

- ACTRIS (Aerosols, Clouds and Trace gases Research Infrastructure), now included in the ESFRI (European Strategy Forum on Research Infrastructures) Roadmap;
- Cloudnet, a network of stations for the continuous evaluation of cloud and aerosol profiles in operational numeric weather prediction models currently integrated into ACTRIS-2;
- the European Union 7th Framework Programme project BACCHUS (Impact of Biogenic versus Anthropogenic emissions on Clouds and Climate: towards a Holistic UnderStanding);
- the COST (European Cooperation in Science and Technology) action TOPROF (Towards operational ground-based profiling with ceilometers, Doppler lidars and microwave radiometers for improving weather forecasts); and
- the COST action PROBE (Profiling the Atmospheric Boundary Layer at European Scale), which began in October 2019.

The interaction with numerous international groups and experts in the framework of these projects is highly beneficial for NUIG in terms of knowledge and experience exchange and it was continued throughout this fellowship.

### ***1.2.6 Provide data to national and international research partners***

As mentioned previously, the synergy of instruments is essential to get a comprehensive view of atmospheric processes. The remote sensing data from Mace Head are therefore used by other scientists at NUIG as well as by external research teams. In the past the data were used in combinations with ground-based and air-borne *in situ* measurements, for satellite validation and for closure studies. This fellowship is aimed at maintaining and intensifying these collaborations.

Throughout the fellowship, data were also directly and automatically transferred to Cloudnet and E-Profile, an EUMETNET (Network of European National Meteorological Services) observation programme that collects measurements from wind profilers and ceilometers in 20 countries.

## **1.3 Structure of This Report**

In the main part of this report, the focus will be on different aspects of atmospheric remote sensing, which were studied in detail during the fellowship period, namely:

- aerosol profiling, including boundary layer detection, profiling of aerosol concentration, transboundary aerosol events and extreme air pollution events;
- cloud profiling, from ground-based remote sensing, models and satellite remote sensing; and
- wind profiling, including a 2-year study on wind characteristics at Mace Head and LLJs.

The following three chapters are structured according to these main themes.



## 2 Aerosol Profiling

For aerosol profiling, the ceilometer is used, which provides a backscattered signal at 1064 nm. This raw signal needs to be corrected and calibrated, as described in section 2.1. In subsequent sections, boundary layer (or more generally aerosol layer) detection (section 2.2), aerosol quantification (section 2.3) and studies of extreme air pollution and transboundary aerosol transport (section 2.4) are discussed.

### 2.1 Ceilometer Calibration

The ceilometer raw signal needs to be corrected for automatic sensitivity changes caused by sunlight or low clouds. These changes in sensitivity protect the receiver part of the ceilometer from damage during times of extreme backscatter signal, but artificially decrease the backscatter signal. As ceilometers were originally developed and used for cloud base detection, this effect was not relevant; however, for aerosol quantification a consistent baseline is required. This correction is made using a factor provided as output from the instrument. After the sensitivity correction, the signal needs to be calibrated from arbitrary units to physically meaningful values in  $\text{m}^{-1}\text{s}^{-1}$  (proportional to photons per m and steradian) using the atmospheric background. For this, a calibration factor was determined from so-called Rayleigh calibrations, where the backscatter signal in a clear atmosphere (no clouds or aerosol) is fitted to the theoretical curve from Rayleigh scattering by molecules using only atmospheric pressure and temperature profiles. Rayleigh calibrations require a few hours of averaging of the ceilometer backscatter signal and these were done periodically, whenever clear night observations provided conditions to obtain the calibration factor. This calibration factor can only be calculated from night-time measurements to avoid solar background radiation causing low signal-to-noise ratios. However, the factor is also applicable during the day and in the case of low clouds because of the stable optical setup of the ceilometer. With the Rayleigh calibration, quantitative information on aerosol layers can be obtained, specifically the backscatter coefficient, as demonstrated in section 2.3.

### 2.2 Aerosol Layer Detection

Using the sensitivity-corrected ceilometer signal, aerosol layers can be detected even without Rayleigh calibration. The layer-detection algorithm is based on changes in the gradient of the signal, i.e. changes along the vertical from low to high signal, indicating the base of a layer, or high to low signal, indicating the top of a layer. Layers, or features, in this context can be aerosol layers or cloud layers. Generally, boundaries of cloud layers are characterised by very sharp signal increases and decreases, hence the primary ceilometer output of cloud base altitude. As mentioned previously, the laser beam sent from the ceilometer cannot penetrate optically thick clouds and therefore the instrument mostly detects the return signal from the cloud base and only a few metres into the cloud. The cloud profile and the cloud top cannot be detected by a ceilometer. However, at Mace Head a cloud radar is collocated with the ceilometer, complementing its output with the in-cloud profile and cloud top altitude. Combining information from both, a feature mask was created, as shown in Figure 2.1.

Grey shades are scaled according to the calibrated ceilometer signal for an approximate estimation of low, medium and high aerosol load. Using the cloud radar, clouds and rain can be clearly detected. On the example day of 10 May 2016, some very small clouds were present until the early afternoon, mostly on top of the high aerosol layer. At around 15:00 Coordinated Universal Time (UTC), a stratiform cloud appeared between 1 and 2 km above ground level (agl), with more small clouds below that layer from around 19:00 UTC onwards. Within the stratiform cloud, rain was detected by the cloud radar, indicating in-cloud drizzle.

Using the ceilometer signal only, the signal gradient can reveal cloud base as well as aerosol layer boundaries. The ABL is defined by dynamic processes; however, with a ceilometer, aerosol load can be used as a proxy. Hence, by observing the vertical aerosol abundance and how it changes with time, the location and extent of the ABL can be inferred. The existing ABL top retrieval algorithm time–height tracking (THT), developed at NUIG (Martucci *et al.*, 2010), processes ceilometer data to detect the tops of the surface mixing

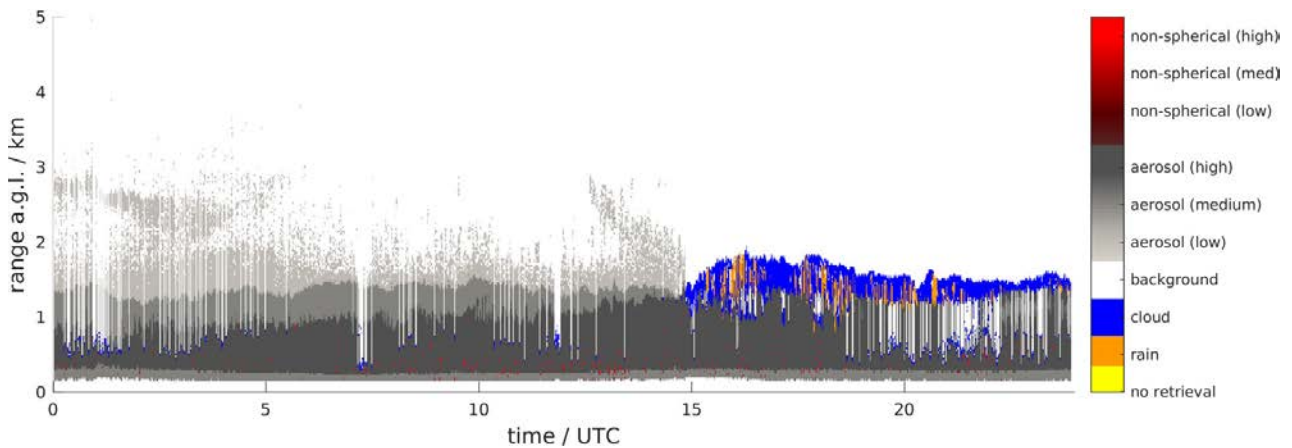


**Figure 2.1. Feature mask combining information from cloud radar – clouds (blue scale), rain (orange scale) and non-spherical large aerosol particles (red scale) – and ceilometer profiles (approximative aerosol load; grey scale) for an example case on 10 May 2016.**

layer, which is the ABL, and a residual layer (RL). Figure 2.2 shows the uncalibrated backscatter signal from the ceilometer (colour), as well as the ABL and RL top altitudes (black and red markers, respectively).

Both ABL and RL tops were captured well by the algorithm. From 15:00 UTC, the RL top follows the cloud, as the strongest gradient in the ceilometer signal is where the laser signal is fully attenuated near the cloud base. From midnight until about 16:00 UTC, when a cloud blocks the detectability of the ceilometer, an aerosol layer was observed even above the RL, in the free troposphere. Such aerosol layers can be transported over long distances, causing transboundary air pollution when they get mixed into the boundary layer. In the case shown in Figures 2.1 and 2.2, the source of this free tropospheric aerosol was probably anthropogenic pollution from continental Europe, according to transport and emission models.

### 2.3 Aerosol Quantification

Quantification of aerosol load from ceilometer measurements is possible given a robust calibration of the instrument and assumptions on the aerosol type. Thanks to extensive studies investigating optical aerosol properties using complex research lidar systems (Müller *et al.*, 2007; Groß *et al.*, 2014; Baars *et al.*, 2016; and many others), the findings can be transferred to routine observations with less sophisticated instruments, such as ceilometers.

In another example of free tropospheric aerosol, on 26 June 2016, layers of high aerosol load were observed starting at 5 km and slowly descending to the RL and ABL. These layers, shown in Figure 2.3, most probably consisted of smoke advected from North American wildfires. In the top panel of Figure 2.3 the backscatter coefficient is shown, which is obtained by correcting and calibrating the ceilometer signal as described in section 2.1. The ratio of extinction-to-backscatter coefficient, or lidar ratio (LR), describes the relationship of backscatter and extinction coefficients and facilitates the calculation of one coefficient from the other. From the lidar literature, the LR can range from 10 to 100 sr, depending on aerosol type, age and source. In continuous automatic operation, these aerosol parameters are generally not known. Therefore, in the automatic retrieval used here, an LR value of 50 sr was assumed, which is a good first approximation for many aerosol types. When the aerosol type and source can be determined for case studies, the LR can be adjusted accordingly. By multiplying the backscatter coefficient with the LR, the extinction coefficient is obtained. Using another conversion factor, the mass-to-extinction ratio (MER), aerosol mass concentration can be calculated from the extinction coefficient. From ground-based *in situ* measurements, Hervo *et al.* (2012) found the MER to be 1.57 g m<sup>-2</sup> for volcanic ash from Eyjafjallajökull and 0.33 g m<sup>-2</sup> for local aerosol measured in central France. Hence, in the example shown in Figure 2.3b, a fixed MER of 0.33 g m<sup>-2</sup> was used. The extinction coefficient profiles are not shown here, as the conversions from

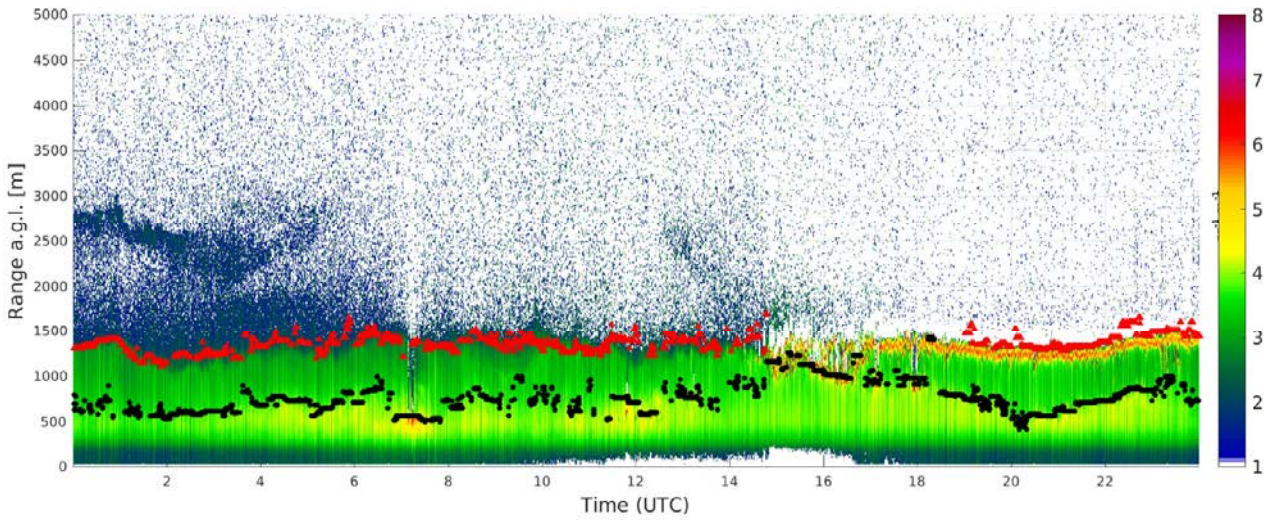


**Figure 2.2.** Uncalibrated ceilometer backscatter signal (colour scale), ABL top (black markers) and RL top (red markers) for the same example case as in Figure 2.1 (10 May 2016).

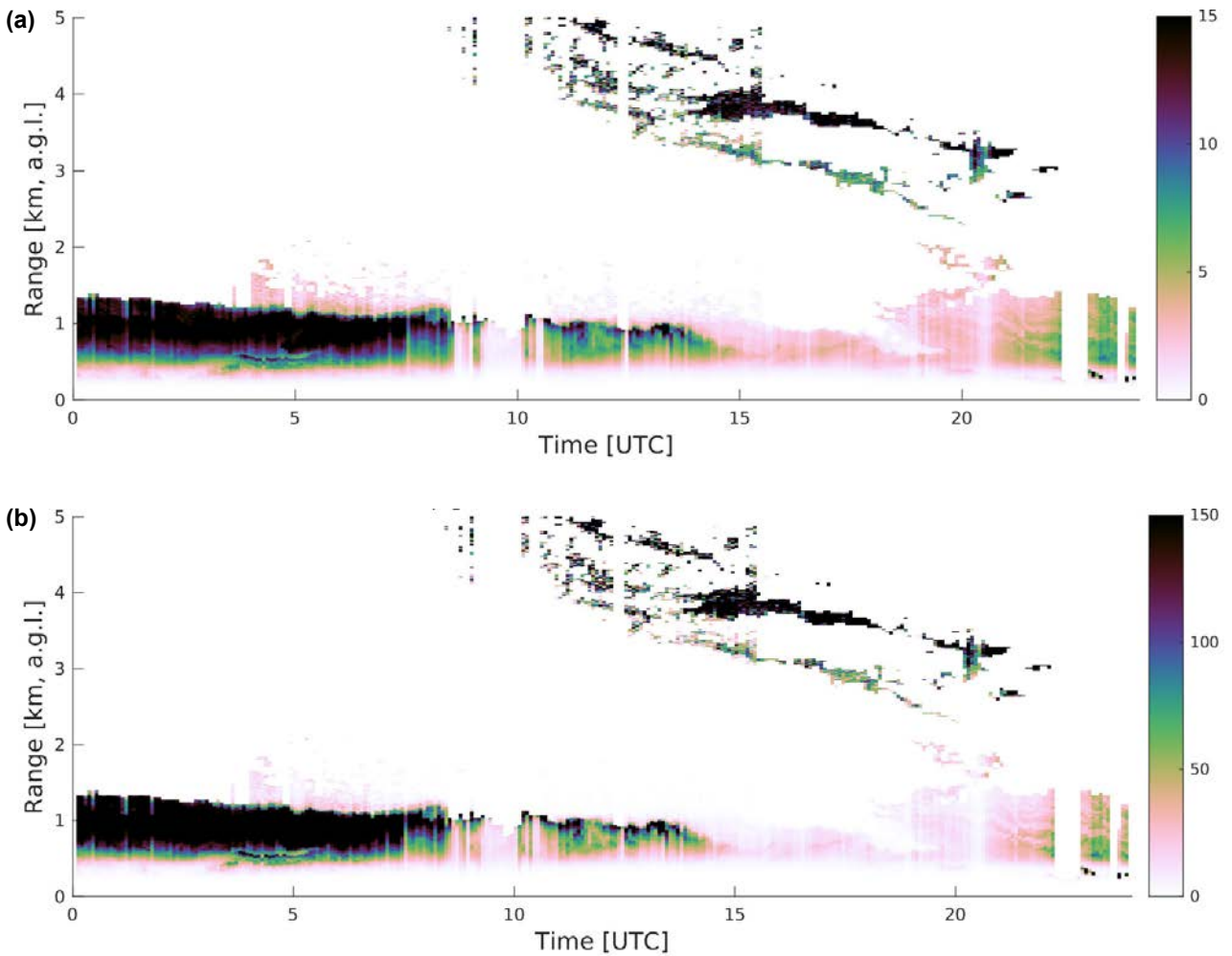


**Figure 2.3.** (a) Time–height display of backscatter coefficient profiles from the ceilometer (in  $M m^{-1} s^{-1}$ ) and (b) aerosol mass concentration profiles (in  $\mu g m^{-3}$ ) over Mace Head, on 26 June 2013.

backscatter to extinction and from extinction to mass concentration are linear procedures and changes in the plots are only a result of the scale.

Both backscatter and mass concentration in Figure 2.3 show long and short periods of profiles of incoherently reduced intensity (e.g. 9:30 to 10:00 UTC, around 20:30 UTC). This is on account of limitations of the algorithm calculating the backscatter coefficient. In addition, the lowest 500m of data are underestimated because of the geometrical setup of ceilometer systems. This geometric effect is constant and can partly be corrected for. In the case shown, the lowest part of the atmosphere cannot be characterised, but in well-mixed conditions the assumption of constant backscatter and mass concentration values from the ground to the top of the mixed layer is valid. Comparison with aerosol number concentration from ground-based *in situ* measurements at Mace Head shows a similar temporal evolution as ceilometer-derived mass concentration at around 800m, with the highest values in the early morning and the lowest values between 15:00 and 18:00 UTC. *In situ* aerosol mass concentration measurements were not available during this time period and further cases will be studied to ascertain the reliability of the remote sensing-derived mass concentration.

## 2.4 Case Studies of Extreme Pollution

In addition to the cases discussed in sections 2.2 and 2.3, some periods of extreme air pollution in Dublin and Mace Head were studied by Lin *et al.* (2018) and Grigas (2017), respectively. For a study of local extreme pollution events in Dublin, on 19 November 2016 and 22 January 2017 (Lin *et al.*, 2018), the ABL top height was calculated from ceilometer data (Vaisala model CL31) from Casement, Dublin, which is about 15km away from the University College Dublin site where *in situ* aerosol observations were recording the pollution levels near the ground. The time resolution of the CL31 is 60s. On 19 November 2016, the ABL thickness was  $230 \pm 75$  m ( $\pm 1$  standard deviation) between 8:00 and 16:00 UTC and  $126 \pm 32$  m between 18:00 and 23:00 UTC, which is  $\sim 1.8$  ( $230/126$ ) times shallower than that during the day. On 22 January 2017, the ABL was  $143 \pm 20$  m during the day and  $134 \pm 14$  m during the evening, which is  $\sim 1.1$  ( $143/134$ ) times shallower than that during the day. Lin *et al.* (2018) found that, even after

accounting for the evening ABL reduction, the evening equivalent black carbon (eBC) concentration was 36–53 times higher than that during the day. The eBC is produced exclusively by combustion processes, such as combustion of fossil fuel and biomass. The coincident increase in eBC and organic aerosol in the evening indicates combustion sources associated with residential heating.

Grigas (2017), on the other hand, studied extreme pollution events (aerosol optical depth  $> 0.5$ ) related to long-range transported aerosols from different sources. The study by Grigas (2017) found about three extreme pollution events recorded at Mace Head using ground-based *in situ* observations only. However, layers with high aerosol load are observed in the free troposphere more frequently and can be missed by ground observations if entrainment into the ABL happens at a later stage. Figures of pollution events detected by remote sensing at Mace Head given in the PhD thesis by Grigas (2017) are reproduced in Figure 2.4 in chronological order: (a) volcanic aerosol from Eyjafjallajökull, Iceland, observed on 19 and 20 April 2010; (b) mineral dust from the Sahara, observed from 7 to 10 April 2011; (c) wildfire smoke from North America, observed from 23 to 26 June 2013 – also mentioned in section 2.3; and (d) anthropogenic pollution from Europe, observed from 12 to 14 May 2016. In addition to remote sensing observations, mass concentrations of absorbing aerosol, such as black carbon (BC) or dust measured at the ground level, are plotted to investigate when entrainment into the ABL occurred. These concentrations are not representative of the overall aerosol load, as non-absorbing aerosols, such as sulfates, nitrates and organic carbon, contribute to the total mass concentration.

In the April 2010 case of volcanic aerosol, only a small amount of absorbing aerosol was entrained into the ABL. The ceilometer signal from the volcanic aerosol layer was highest on 19 April 2010 at around 3 km agl and the layer descended gradually until it was entrained into the ABL in the evening of that day, with a small increase in mass concentration of absorbing aerosol around midnight. More absorbing aerosol was mixed down to the ground level during the observation of Saharan dust in April 2011, when the pollution event at the ground level lasted several days. BC from wildfires in North America observed in June 2013 led to rather short, but very intense, spikes

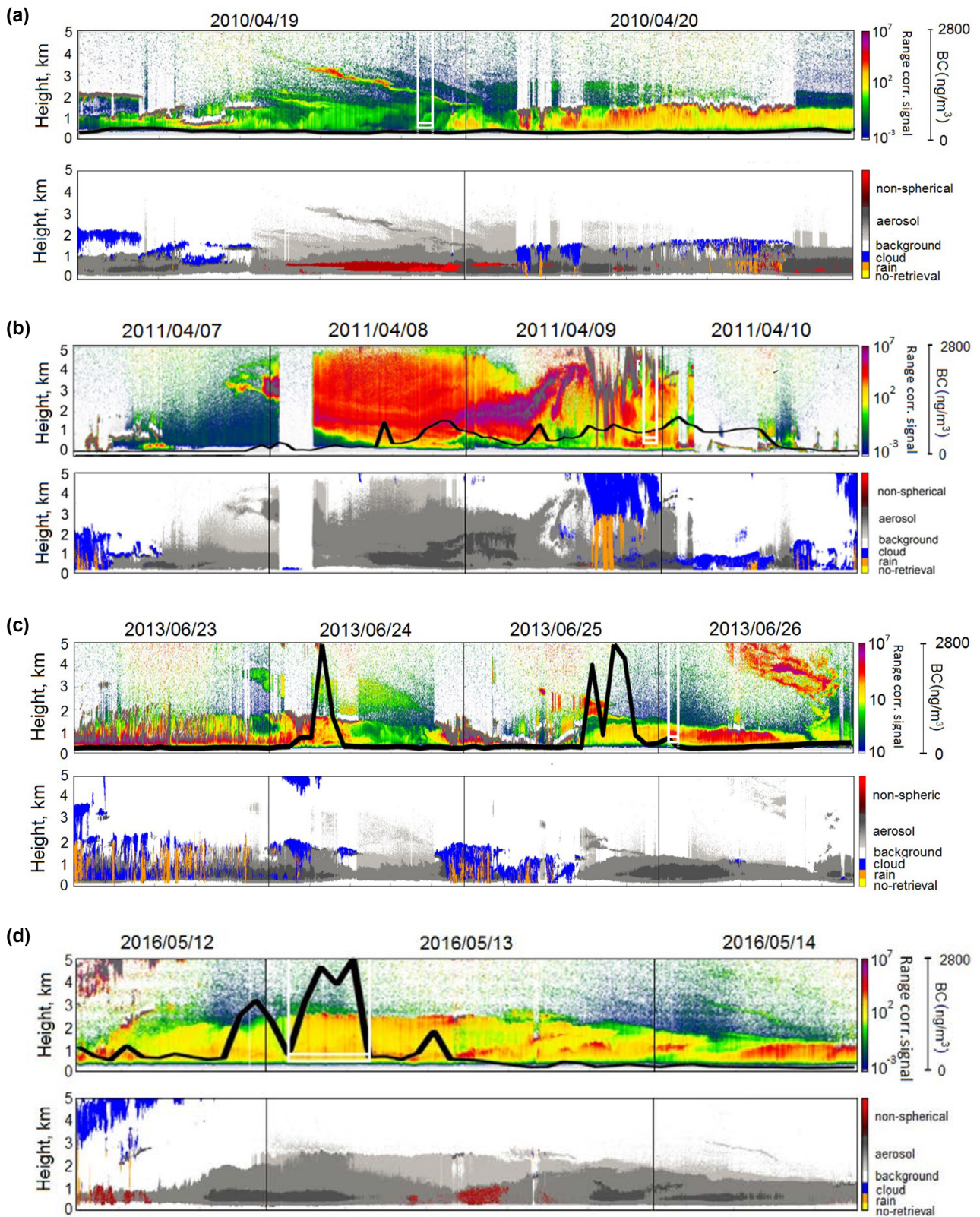


**Figure 2.4.** Ceilometer signal (top panels, colour scale), mass concentration of absorbing aerosol (BC or dust – top panels, black line), feature mask (bottom panels) for four episodes of extreme air pollution at ground level, or high aerosol load in the free troposphere, of different aerosol types and from different sources. (a) Volcanic aerosol from Eyjafjallajökull, Iceland; (b) mineral dust from the Sahara; (c) wildfire smoke from North America; (d) anthropogenic pollution from Europe.

in ground-level mass concentration. Anthropogenic aerosol from Europe also carried high BC levels to Mace Head, in an event that lasted for a period of over 12 hours.

Table 2.1 (adapted from Table 19 and Figure 56 in Grigas, 2017) lists volume and mass concentrations from *in situ* observations as well as integrated backscatter (IBS) from the ceilometer during time periods marked as white boxes in Figure 2.4. The IBS was derived from the corrected ceilometer signal, which is integrated over two different altitude ranges (0.6–0.8 km and 0.8–5 km) and normalised by the depth of the layer (0.2 and 4.2 km, respectively).

The May 2016 case of anthropogenic pollution showed the highest impact on ground-level volume and mass concentrations, probably because of the closeness of the aerosol source region (continental Europe) to Mace Head. However, in terms of aerosol load aloft, the Saharan dust case shows the highest values of IBS in both integration ranges. This finding shows that

aerosol load aloft can be decoupled from ground-level concentrations, but cannot be neglected, as whatever pollution is suspended will eventually reach the ground. In all selected time periods shown in Table 2.1, the aerosol load represented by normalised IBS in a layer between 0.6 and 0.8 km was considerably larger than in the layer above.

## 2.5 Copernicus Atmosphere Monitoring Service Validation

In the framework of E-Profile, an EUMETNET observation programme, ceilometer data from Mace Head are shared continuously and used for comparison with CAMS forecasts. Observation-background statistics for Mace Head and other locations throughout Europe are shown in Figure 2.5 (from an internal E-Profile report, labels removed). There, CAMS forecast backscatter coefficients are compared with backscatter coefficients measured by ceilometers.

**Table 2.1. Volume and mass concentrations from ground-based *in situ* measurements and normalised layer IBS from ceilometer measurements for four case studies**

| Case                              | Volume ( $\mu\text{m}^3 \text{cm}^{-3}$ ) | Mass ( $\mu\text{g m}^{-3}$ ) | IBS (0.6–0.8 km) | IBS (0.8–5 km) |
|-----------------------------------|---|-------------------------------|------------------|----------------|
| April 2010: volcanic ash          | 32.67                                     | 46.71                         | 60               | 30             |
| April 2011: Saharan dust          | 20.33                                     | 50.83                         | 250              | 120            |
| June 2013: wildfire smoke         | 8.88                                      | 17.86                         | 170              | 30             |
| May 2016: anthropogenic pollution | 64.67                                     | 99.97                         | 150              | 30             |

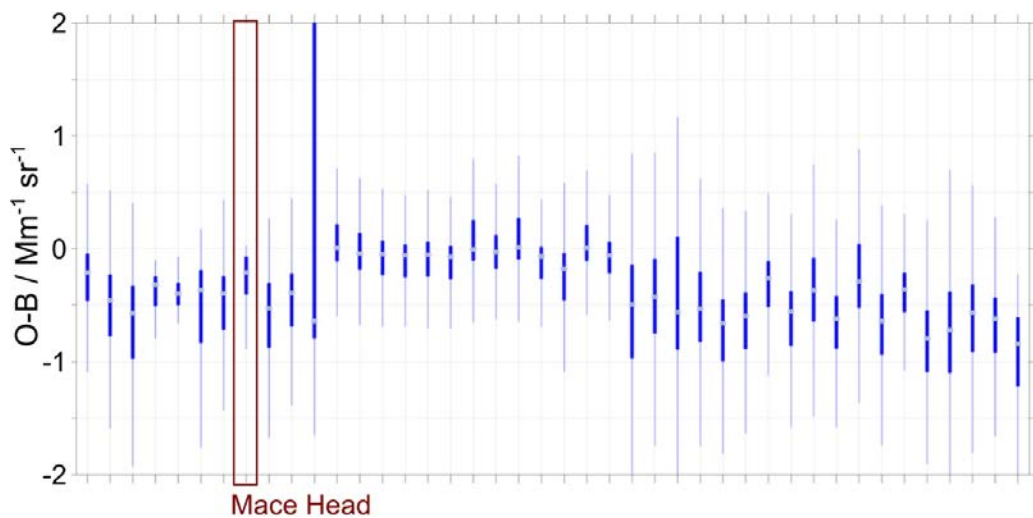


**Figure 2.5. Observation-background (O-B) statistics comparing CAMS forecasts with ceilometer measurements for August 2019 from the monthly E-Profile report. Station labels of other locations have been removed; the Mace Head ceilometer comparison is highlighted by a maroon box.**

The example in Figure 2.5, from August 2019, showed a bias of  $-0.2 \text{ M m}^{-1} \text{ s}^{-1}$  for the ceilometer at Mace Head, which is small in absolute terms compared with

ceilometer data from other locations. In addition, the range of backscatter difference throughout the month (thin vertical line) at Mace Head is among the smallest.

### 3 Cloud Profiling

Aerosols play an important and anthropogenically altered role in the radiative budget of the planet, as does the impact of clouds on solar radiation, which cannot be neglected. The impact of clouds on solar radiation is highly variable and strongly linked to aerosol concentration and type. In general, the effective radius of cloud droplets is smaller in clouds affected by polluted air masses than in clean clouds (Lohmann and Feichter, 2005, and references therein). This effect was also observed by Ferek *et al.* (2000), who investigated marine clouds influenced by ship emissions. They also found drizzle suppression in ship tracks. Rosenfeld *et al.* (2008) discussed the role of aerosol particles as cloud condensation nuclei (CCN) and their ambivalent impact on precipitation, namely, on the one hand, evaporation or prevention of clouds in heavily polluted conditions and, on the other hand, prevention of long-lived clouds in the tropics on account of clean conditions and fast rainout. A review of publications discussing marine and continental stratiform clouds was carried out by Miles *et al.* (2000). They found clear differences between these two types in terms of total CDNC, effective cloud droplet diameter and LWC, among other things.

#### 3.1 Cloud Properties

The algorithm SYRSOC was developed at NUIG by Martucci and O'Dowd (2011) to provide the microphysical cloud properties of CDNC, effective cloud droplet radius ( $r_{\text{eff}}$ ) and LWC, as well as the optical cloud properties of COT and cloud albedo from data obtained by ceilometers, cloud radars and microwave radiometers. During this fellowship period, novel implementation and validation of SYRSOC in fog cases led to improvements of the algorithm. In this fog study, data from instruments located at the Atmospheric Research Observatory at Palaiseau near Paris, SIRTa (Site Instrumental de Recherche par Télédétection Atmosphérique), were used. The implementation of SYRSOC at SIRTa facilitates the study of clouds under continental influence, as well as that of fog. Profiles of cloud microphysical properties in very low clouds and especially in fog are also obtained from *in situ* measurements with tethered balloons at SIRTa, carrying a granulometer (light optical aerosol

counter – LOAC) measuring profiles of cloud droplet size distribution between 0.2 and 50  $\mu\text{m}$  *in situ* and a diffusometer (Degreane DF320) measuring horizontal visibility. Part of this study was aimed at evaluating SYRSOC's performance against those *in situ* profiles, which provide an independent reference. SYRSOC was applied to data from the following SIRTa instrumentation: backscatter signal from CHM15k (Lufft, Germany) and CL31 (Vaisala, Finland) ceilometers to detect cloud base; reflectivity from the BASTA (Bistatic Radar System for Atmospheric Studies) cloud radar (built at SIRTa) to detect cloud top and to calculate CDNC, combined with information from the other instruments; a HATPRO (Humidity and Temperature Profiler) microwave radiometer (RPG, Germany), which measures the LWP; and *in situ* mast measurements of temperature, assuming an adiabatic temperature decrease with height above the mast.

The CDNC,  $r_{\text{eff}}$  and LWC from SYRSOC were compared with three fog profiles from two different balloon measurements, on 6 January 2015 and 19 December 2016. The initial comparison revealed not only limitations of SYRSOC but also ways of improving the algorithm. This fog study was published by Dupont *et al.* (2018).

The cloud base in any fog layer is at the ground level; however, similar to most cloud radars, BASTA has a blind zone in the lowest 40 m and reflectivity below 240 m is reduced on account of the geometrical setup of the radar (Delanoë *et al.*, 2016). On the other hand, the LWP of the whole column is measured by HATPRO. In case of fog, much of the liquid water will be located in the lowest 240 m. Therefore, BASTA reflectivity was corrected in the height range of 120–240 m using a near-field correction proposed by Sekelsky (2002). Below 120 m, reflectivity was assumed to be constant, using an average value. Such a correction will be necessary for most cloud radar systems before applying SYRSOC in fog layers.

In the analysed fog cases, the vertical resolution of HATPRO temperature profiles caused further difficulties as a result of inversions, which were not captured. Hence, instead of the HATPRO temperature profiles, the standard input of SYRSOC, temperature



profiles were derived from *in situ* mast measurements. Above the mast, an adiabatic temperature decrease with height was assumed. At higher altitudes, radio sounding provided a good match to HATPRO temperature data.

Finally, an entrainment factor was introduced to take into account entrainment of dry air at the cloud/fog layer top. The entrainment factor is calculated for the top 30% of the cloud, replicating the shape of the measured reflectivity profile. The ratio of radar reflectivity at each height bin to radar reflectivity at 30% from the cloud top is calculated. This height-dependent factor is then multiplied by the CDNC profile to produce more realistic shapes of the CDNC profile and subsequently of  $r_{\text{eff}}$  and LWC profiles. The implementation of an entrainment factor was an overall improvement of SYRSOC, not only for fog cases.

The combined effect of all these improvements is shown in Figure 3.1, illustrating differences between the initial and improved SYRSOC versions. CDNC and  $r_{\text{eff}}$  profiles of the improved SYRSOC agreed very well with LOAC measurements in the lower half of the fog layer, where LOAC profiles were available. Both

BASTA profiles overestimate  $r_{\text{eff}}$  and underestimate CDNC compared with LOAC profiles. BASTA LWC matches LOAC LWC very well for coincident measurements (dashed orange line). The average BASTA LWC profile for the whole period is slightly higher, as is the SYRSOC LWC. In addition, there is an increasing difference with height above the cloud centre between the BASTA and SYRSOC LWC.

None of the corrections fully accounted for deviations in the BASTA and SYRSOC LWC profiles. An overestimation of LWC by SYRSOC in the top half of the fog layer was observed in all cases studied by Dupont *et al.* (2018). SYRSOC produces the linear LWC increase expected in water clouds, modified at the top by the entrainment factor. However, the shape of the LWC profile in fog depends on the phase in the fog life cycle – formation phase, mature phase and dissipation phase. LWC gradients in fog can be positive, quasi-null or negative and they depend on a number of factors, such as evaporation at the cloud top, precipitation or sedimentation at the cloud base, evaporation at the cloud base, and temperature and humidity gradients above the fog top. As the

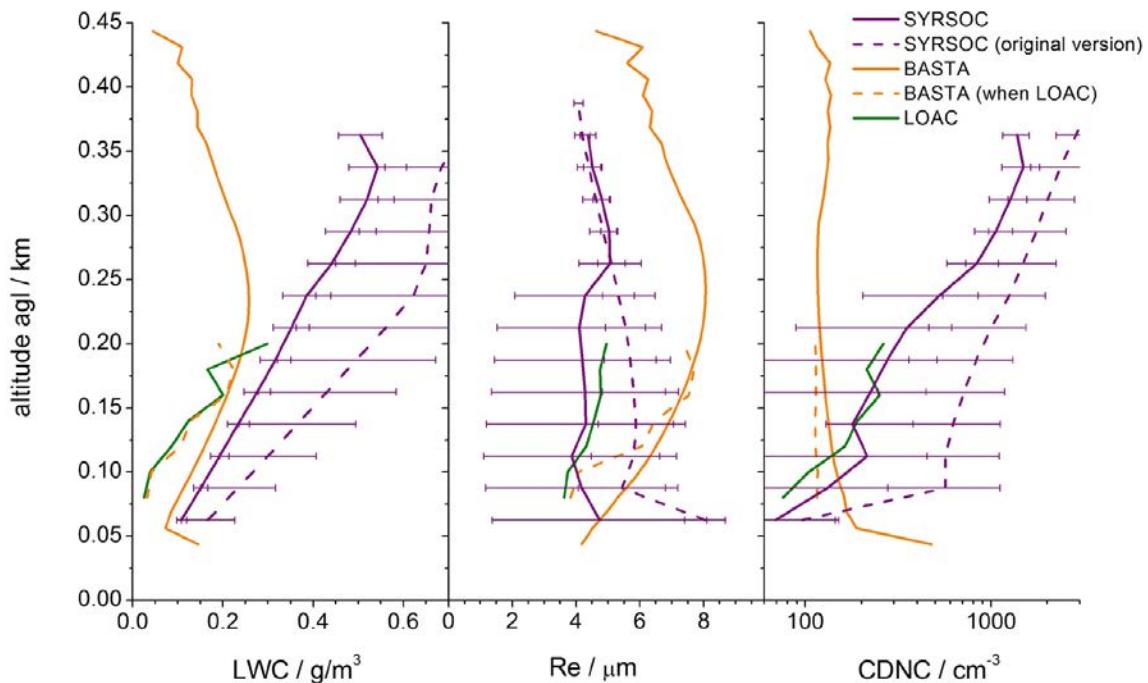


**Figure 3.1. Vertical profiles of LWC (left),  $r_{\text{eff}}$  (Re in plot, centre) and CDNC (right) derived from LOAC (green), BASTA (orange) and initial (dashed purple line) and improved (solid purple line) SYRSOC versions. For BASTA, measurements coincident with LOAC (dashed orange line) were distinguished from those averaged over the complete sampling period (solid orange line). The sampling period was 6 January 2015 between 14:00 and 15:00 UTC. Error bars on SYRSOC profiles indicate standard deviation of the mean over the 1-h period.**

fog thickness is limited to some hundreds of meters, those competitive processes have a significant impact on the LWC profile throughout the fog layer. None of these factors is taken into account in SYRSOC, which explains differences between LOAC/BASTA and SYRSOC profiles, not only of LWC, but also of CDNC and  $r_{\text{eff}}$ .

### 3.2 Cloud Parcel Model

Aerosols are known to alter liquid water, ice and mixed-phase cloud formation processes, CDNC and precipitation from warm clouds, thereby causing an indirect radiative forcing associated with these changes in cloud properties. However, the determination of the global cloud radiative forcing and the impact of aerosols on it is affected by large uncertainties, especially concerning the lifetime effect (longer cloud lifetime because of suppressed precipitation) and the droplet size distribution (Stocker *et al.*, 2013).

A Fortran-based cloud parcel model (O’Dowd *et al.*, 2000) was set up to better investigate the link of microphysical cloud properties to aerosol events. This model determines activation of CCN to cloud droplets, using sea salt and SO<sub>4</sub> size distributions as input. In addition to SO<sub>4</sub> and sea salt size distributions, CDNCs were obtained independently from *in situ* measurement data. These observational data (“Amb”) and Fortran model results (“Model”) are shown in Table 3.1 for different air masses. Details on air masses were given by Fossum *et al.* (2018). There is good closure for continental polar (CP) air masses. Comparisons showed an acceptable level of agreement, with differences of less than 25%. The CP data found closure using the Aitken mode fitting at 0.13 m s<sup>-1</sup> updraft. However, there were discrepancies between modelled and measured data for marine polar (MP) air masses. Although sea salt and SO<sub>4</sub> CDNCs

were very well represented by the model, the modelled and observed supersaturations show a large difference of 64.4%.

This is the first step towards validating the model results with SYRSOC CDNCs. However, the search for cases for comparison is complicated by restrictions of suitable clouds for SYRSOC and of suitable periods for the retrieval of cloud model input. In particular, the requirement for precipitation- and drizzle-free clouds of SYRSOC is rarely met in stratiform clouds in the marine environment of Mace Head when *in situ* aerosol consists mostly of SO<sub>4</sub> and sea salt.

### 3.3 Ground- and Satellite-based Remote Sensing of Clouds

For a combination of ground- and satellite-based remote sensing of clouds, data from the SEVIRI onboard the MSG (Meteosat Second Generation) satellite was used in this study. SEVIRI observes the atmosphere in 11 channels with 3-km spatial resolution at nadir and 15-minute temporal resolution. The cloud top height (CTH) product used here is part of the MSG CPP (Cloud Physical Properties) products from the Royal Netherlands Meteorological Institute (KNMI; Roebeling *et al.*, 2006). In the KNMI’s approach, CTH was derived from cloud top temperatures measured by SEVIRI. In Figure 3.2 a comparison of CTH from satellite-based SEVIRI and ground-based cloud radar at Mace Head is shown for two example cases on 11 and 12 June 2017. During the study period, the presence of varying clouds as well as multiple cloud layers posed a challenge in comparing results from ground-based radar with those from a satellite-based imager. On one hand, good significant correlation of CTH was observed on 11 June 2017, but with a large and mostly consistent bias, with SEVIRI overestimating CTH. The comparison on 12 June 2017 shows larger variability and periods with better, but

**Table 3.1. Comparison of measured (Amb) and modelled (Model) CDNC and supersaturation (sup\_max) from the Fortran model for CP and MP air masses**

|  | CP   |        |                | MP     |        |                |
|--|------|--------|----------------|--------|--------|----------------|
|  | Amb  | Model  | Difference (%) | Amb    | Model  | Difference (%) |
| updraft/m/s                            | –    | 0.13   | –              | –      | 0.13   | –              |
| sup_max                                | 0.34 | 0.3407 | 0.2            | 0.2044 | 0.3361 | 64.4           |
| CDNC SS/cm <sup>-3</sup>               | 2    | 1.67   | 16.5           | 13     | 14.5   | 11.3           |
| CDNC SO <sub>4</sub> /cm <sup>-3</sup> | 185  | 144.17 | 22.1           | 140    | 135.9  | 2.9            |

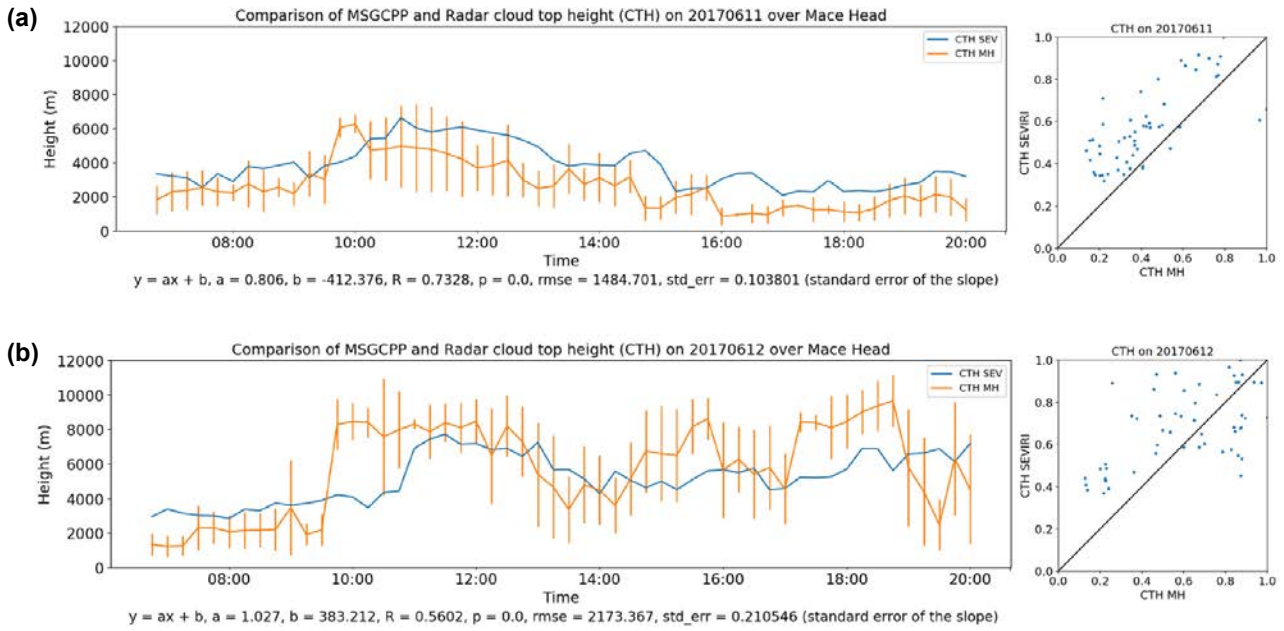


**Figure 3.2. Comparison of CTH from satellite-based SEVIRI and ground-based cloud radar at Mace Head on (a) 11 June 2017 and (b) 12 June 2017.**

also with worse, agreement. Overall, correlation on 11 June 2017 was stronger than on 12 June 2017, with  $R$  of 0.73 and 0.56, respectively. In a more detailed

future study, the cloud classification product from SEVIRI could be useful to find systematic deviations, depending on cloud type.

## 4 Wind Profiling

Wind characteristics – such as horizontal wind speed and direction and turbulence – and their seasonality and occurrence are crucial information for wind and wave energy production. In particular, turbulence and wind shear are important parameters for the wind energy sector, as they can put enormous stress on turbines (Shen *et al.*, 2011). They also play an important role in aviation safety, as rapid strong changes in headwind caused by turbulence or shear can lead to critical situations, especially during take-off and landing (ICAO, 2018). Turbulence and wind shear are linked not only to certain meteorological conditions, but also to topography. The scale of atmospheric turbulence, or the size of eddies, can vary from macroscale to microscale. The size of eddies that are most relevant for aviation safety is about 100 m to 1 km (Sharman and Lane, 2016). This is a scale that the Doppler lidar can cover, with its radial resolution of 75 m and detection range of more than 10 km. Eddy dissipation rate (EDR) is a measure for turbulence, and vertical wind shear is the change in horizontal wind speed or direction along the vertical profile. Both parameters are provided automatically and continuously from wind lidar measurements at Mace Head.

Low-level jets are wind speed maxima along the vertical profile in the lower levels of the atmosphere, mostly observed from evening to late morning. In standard atmospheric conditions, the wind speed logarithmically or linearly increases with increasing altitude. In the case of an LLJ, local wind speed maxima occur along the vertical profile. These jets can have a two-sided effect on wind turbines. On the one hand, a higher wind speed at turbine altitude will increase energy production, up to a certain threshold where efficiency decreases again (Hirth and Müller, 2016); on the other hand, strong wind speed maxima are associated with higher wind shear and turbulence, which causes stress on turbines and thus reduces their efficiency and lifetime (Wagner *et al.*, 2011; Kumer *et al.*, 2016).

### 4.1 Wind Lidar Data Processing

In the framework of this fellowship, an extensive processing software package to scan Doppler wind lidar data was developed. The standard outputs of the instruments are profiles of radial wind speed and CNR along the line of sight (LOS). From those, the WindCube software package, developed in Python, calculates the following parameters automatically at hourly intervals:

- vertical profiles of horizontal wind speed;
- vertical profiles of horizontal wind direction;
- vertical profiles of vertical wind speed shear – change of wind speed per 100-m altitude;
- vertical profiles of vertical directional shear – change of wind direction per 100-m altitude.

In addition, it converts the text-based output files of the lidars to a NetCDF format containing metadata and produces plots of observations at all scan patterns. The WindCube package is schematically illustrated in Figure 4.1. Details on the retrieval of its products are given in sections 4.1.1–4.1.4.

The output of the WindCube package is automatically fed into algorithms for calculation of EDR, developed at the University of Reykjavik in collaboration with the Icelandic and Finnish weather services (the Icelandic Meteorological Office – IMO – and the Finnish Meteorological Institute – FMI; Yang *et al.*, 2019), and for detection of LLJs, developed at FMI (Tuononen *et al.*, 2017).

In addition to these routine products, attenuated backscatter profiles were produced on a case study basis. This feature is in the development stage and has not yet been fully tested.

#### 4.1.1 Data quality screening

The quality of radial wind data influences the uncertainties in the resulting wind profiles, which propagate to all other wind products. Before calculating further products, radial wind data were therefore screened for noise and otherwise invalid

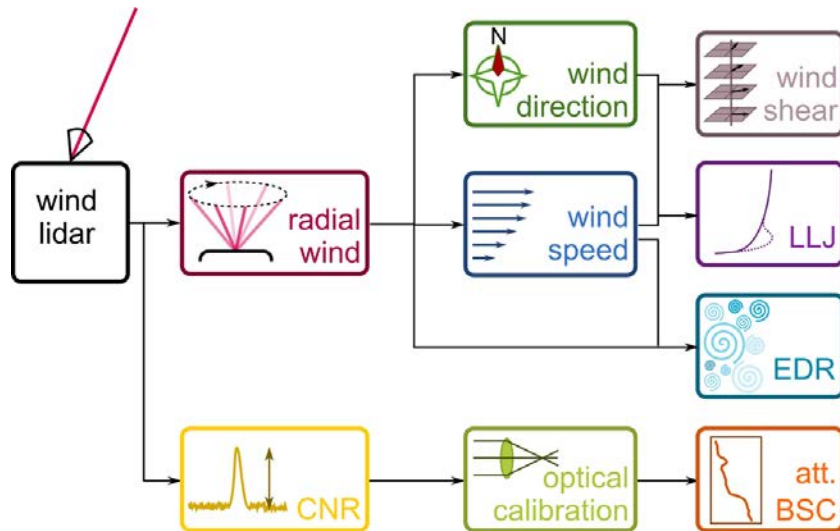


**Figure 4.1. Flow chart of the WindCube Doppler lidar output and all products generated by the Python-based WindCube software package. Att. BSC, attenuated backscatter.**

data points. For that purpose, a confidence index (Clx) was applied, which is the output of the instrument in addition to radial wind and CNR data. Radial wind at each time- and range-step was determined by computing the spectrum using a fast Fourier transform method and subsequently fitting this spectrum to a theoretical curve. The Clx threshold depends on CNR, mean error and spectrum broadening of this spectral fit. It is factory calibrated individually for each instrument and each range gate length. The calibration requires a few hours of noise measurements, whereby outgoing radiation is shielded from the receiver telescope. The Clx threshold is then set to a value that limits the false-positive rate to 0.25%. Clx is a binary quality control parameter of value 0 for rejected data points and 100 for valid data points.

For one of the Doppler lidars, this Clx was tested against various CNR thresholds proposed by Päsche *et al.* (2015), Manninen *et al.* (2016) and Tuononen *et al.* (2017) as well as by other researchers who used Doppler lidar models from a different manufacturer (Halo Photonics). Data availability for full velocity azimuth display (VAD) scan profiles at a 15° elevation angle on an example day (26 February 2018) depending on CNR thresholds and Clx are shown in Table 4.1. Clx combines a CNR threshold with other goodness-of-fit parameters. Using Clx, higher data availability was achieved than by applying a simple CNR threshold of less than -25 dB. Most commonly, CNR thresholds of more than -22 dB are used.

#### 4.1.2 Retrieval of vertical profiles of horizontal wind

Profiles of horizontal wind speed and direction were obtained from conical scans, which are also referred to as VAD scans. VAD scans are conical scans at fixed elevation angles, consisting of 12 beams, at constant azimuthal angles 30° apart. Within each hour, four VADs were performed at 15° elevation with 2 seconds at each discrete azimuthal position, followed by VADs at 75° elevation with 5 seconds at each azimuthal position. Additionally, VAD scans at 4° elevation were introduced in May 2018, with 2 seconds at each discrete azimuthal position. Figure 4.2 illustrates the principle. Assuming horizontal homogeneity of the wind field around the cone, the radial wind follows a sine or cosine shape. Therefore, a least square fit of the radial wind at 12 points was applied to the following function:

$$y = a + b * \cos(\theta^* - \theta_{\max}) \quad (4.1)$$

with  $a$ ,  $b$  and  $\theta_{\max}$  being the offset, amplitude and phase shift of the cosine, respectively, and  $y$  and  $\theta^*$  being the radial wind velocity and azimuth angle, respectively. An iterative process determined the optimum solution of  $a$ ,  $b$  and  $\theta_{\max}$ . Horizontal wind speed  $u$  was calculated as follows:

$$u = \frac{b}{\cos(\phi)'} \quad (4.2)$$

**Table 4.1. Data availability depending on CNR thresholds, tested on full profiles of VAD scans at a 15° elevation angle, over 24 hours on the example day 26 February 2018**

| CNR threshold (dB) [ratio] | Data availability (%) | Previous studies (examples, where available)                 |
|----------------------------|-----------------------|--|
| -18.2 [0.015]              | 18                    | Päschke <i>et al.</i> (2015)                                 |
| -21 [0.008]                | 22                    | Manninen <i>et al.</i> (2016); Tuononen <i>et al.</i> (2017) |
| -22 [0.006]                | 22                    | Manninen <i>et al.</i> (2016)                                |
| -25 [0.003]                | 24                    |  |
| -30 [0.001]                | 32                    |  |
| Cix=100                    | 24                    |  |

For comparison, data availability based on Cix used in this study is given in the last row.

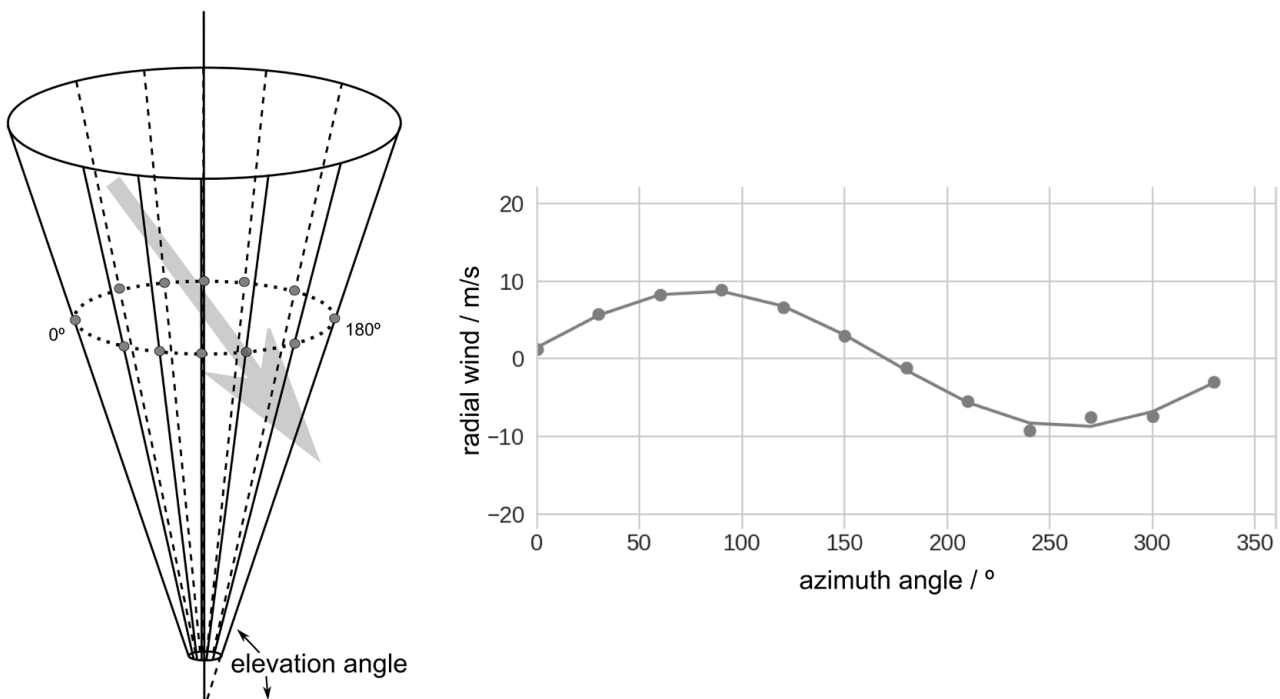


**Figure 4.2. Schematic illustration of the VAD scan pattern with 12 beams and sine fit procedure to obtain horizontal wind speed and direction. Horizontal wind is shown as the big arrow and radial wind values along each of the 12 beams are shown as dots.**

with  $\phi$  being the elevation angle. Horizontal wind direction  $\theta$  equals the least square solution of  $\theta_{\max}$ .

The VAD scans were performed at three different elevation angles. Scans at large elevation angles sample a volume close to the central axis, decreasing the influence of horizontal inhomogeneity in the wind field, whereas scans at low elevation angles return the wind field at a higher vertical resolution. For the Mace Head Doppler wind lidars at their current settings, the first range bin was at 150-m distance from the lidar. This corresponds to an altitude above the instrument

of 145 m, 39 m and 10 m at elevation angles of 75°, 15° and 4°, respectively. Based on the range resolution of 75 m, the effective vertical resolutions for the three scan angles were 72.5 m, 20 m and 5 m, respectively.

The described approach works under the assumption of horizontal homogeneity of the wind field within the circumference of the sampled cone. This can introduce uncertainties in case of highly turbulent or low-wind periods, which is reflected in the fit quality. Fit results were screened using Pearson's correlation coefficient  $R$ , following Päschke *et al.* (2015), who used a

threshold of 0.95 for  $R^2$ . The optimum threshold for the dataset presented here was an  $R$  of 0.98, which corresponds to an  $R^2$  of 0.96. Additionally, missing or rejected data points were taken into account. Only fits with a minimum of 8 out of 12 data points were included for further analysis.

#### **4.1.3 Wind profiles from the Weather Research Forecast model**

Doppler wind lidars are ideal to observe the wind at high temporal and vertical resolution; however, they are limited to one geographical location. Atmospheric high-resolution models can help to forecast wind profiles over any location required, while Doppler lidar profiles can be used to validate model information or even to act as input into the model. The Weather Research Forecast (WRF) model is run operationally at NUIG, underlying the StreamAIR air quality forecast, available online at <http://streamair.nuigalway.ie/> (accessed July 2019). The WRF model is run at three different horizontal resolutions on nested grids of 1-, 5-, and 25-km grid size. The model provides profiles of horizontal wind speed and direction, among other parameters. This wind information can be used to study the temporal and spatial (four-dimensional) extent and development of wind fields, including LLJs. Furthermore, wind profiles are automatically extracted from the gridpoint nearest to Mace Head.

#### **4.1.4 Low-level jet detection**

Automatic and continuous LLJ detection in Doppler wind lidar profiles was implemented using an algorithm developed by Tuononen *et al.* (2017). Up to four local wind maxima can be detected in each vertical profile. A tracking approach ensures consistency of the output by discarding spurious false detections on account of noisy data. In addition to wind lidar profiles, this LLJ detection algorithm was adapted to analyse vertical wind profiles from the WRF model.

## **4.2 Wind Characteristics at Mace Head**

A 2-year dataset of automatic and continuous wind lidar measurements from 1 January 2017 to 31 December 2018 was analysed. There were short gaps in observations because of power cuts, as well

as data acquisition or storage problems. Here, data gaps are considered to be when full wind profiles are missing, unlike gaps along the vertical profile. The latter occurred frequently as a result of meteorological conditions, such as a low concentration of scatterers or the presence of fog or clouds. Gaps also occurred after applying quality filters during times of high turbulence, which can lead to inhomogeneous conditions and, consequently, poor horizontal wind data quality (section 4.1.2). Condensation on the telescope window occasionally led to a very poor CNR and missing data, both along the vertical profile, as well as of full profiles.

Theoretically, four wind profiles should be available per hour, corresponding to four scheduled VAD scans. Quality screening of wind profiles had little impact on availability of full wind profiles. Overall availability of analysed VAD scan profiles per year was 78% in 2017 and 89% in 2018. For 2017, screening reduced the dataset by 1% to 77%. There was no change for 2018. The quality screening is applied to each profile and range bin individually. Therefore, not many full profiles have been removed, but only certain range bins.

Figure 4.3a shows a box plot of the distribution of horizontal wind speed per month from lidar at the lowest range bin (39 m). Each month represents a minimum of 3174 data points (February) and up to 5619 data points (May). A clear seasonality was observed in measured horizontal wind speed, which was higher in winter (highest median of  $11 \text{ m s}^{-1}$  in January) and lower in summer (lowest median of  $7 \text{ m s}^{-1}$  in July).

The interquartile range of distributions, which is the difference between the 75th and 25th percentiles, was largest in January (about  $8 \text{ m s}^{-1}$ ) and lowest in July and August (about  $5 \text{ m s}^{-1}$ ), indicating higher and lower variability, respectively. Figure 4.3b shows the distribution of horizontal wind direction, from lidar measurements at 39 m. The average horizontal wind direction was obtained by vector averaging. Wind direction is here referred to as wind-from direction, with  $0^\circ$  and  $360^\circ$  being north. Generally, wind from the west-south-west was dominant. Studying a 3-year period of 10-m wind measurements at Mace Head, Jennings *et al.* (2003) found a prevailing wind direction between  $180$  and  $300^\circ$ , with air arriving from that sector 51% of the time. The fraction of wind coming

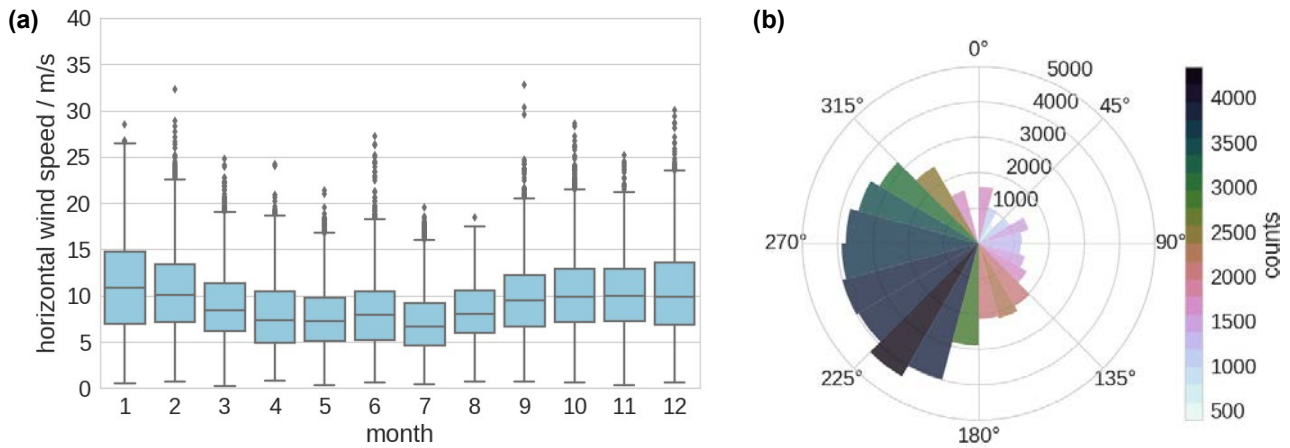


**Figure 4.3. (a) Monthly distributions of horizontal wind speed and (b) distribution of horizontal wind direction (right) from Doppler wind lidar at the lowest range bin at 39 m agl from 2 years of observations. Boxes represent the 25th and 75th percentiles, horizontal lines are medians, whiskers show 1.5 times the interquartile range (difference between 75th and 25th percentiles) and diamond markers are data points outside that range. The polar plot shows counts binned in 15° sectors.**

from this sector measured by lidar during this 2-year period was 55%.

#### 4.2.1 Low-level jet characteristics

The LLJ detection for both years yielded the monthly occurrence, LLJ peak wind speed and peak altitude, as well as the distribution of wind direction at peak altitude, shown in Figure 4.4. The numbers of LLJs observed per month during the 2-year period are given in the top plot. In total, 237 LLJs were detected. Most LLJs were observed from March to June. In August and September, LLJ numbers were – with 4 and 6, respectively – not sufficient to obtain statistically significant information. Median values of peak altitude,

shown in Figure 4.4b, did not change much throughout the year. Most LLJs were detected between 100 and 400 m agl, which is an altitude range relevant for large wind turbines with hub heights of around 100 m or more and rotor spans of around the same extent. Median peak wind speed was slightly lower in summer than in winter, with the exception of January. Peak horizontal wind speed ranged mostly from 5 to 15  $\text{m s}^{-1}$ .

The LLJs were predominantly observed from the east. On the other hand, Figure 4.3 shows a prevailing westerly flow at Mace Head. This allows the conclusion that, at Mace Head, LLJs are associated with easterly conditions, which are linked to high pressure systems and which are less common there.



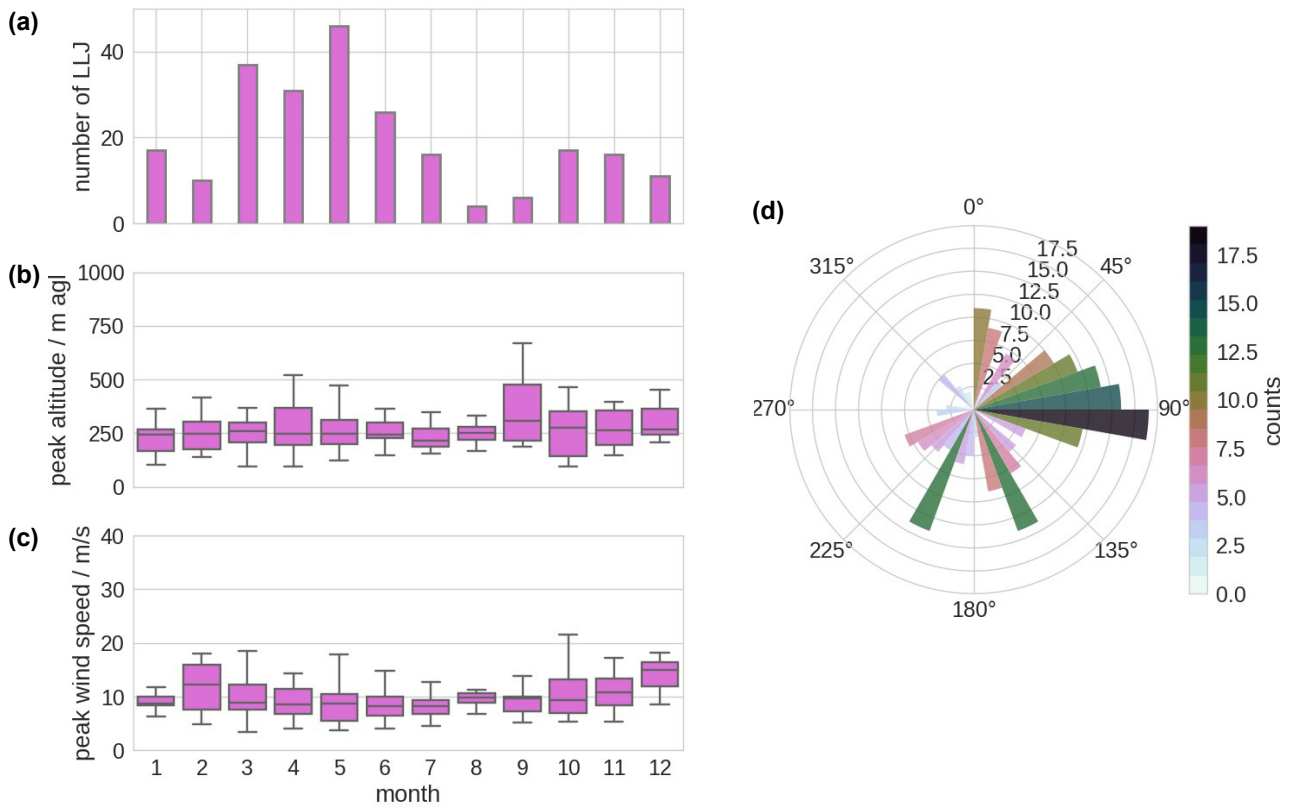


**Figure 4.4.** LLJ (a) number, (b) peak altitude, (c) peak wind speed and (d) peak wind direction from 2 years of Doppler wind lidar observations. Boxes represent the 25th and 75th percentiles, horizontal lines are medians, whiskers show 1.5 times the interquartile range (difference between 75th and 25th percentiles) and diamond markers are data points outside that range. The polar plot shows counts binned in 15° sectors.

## 5 Summary and Recommendations

This fellowship focused on continuous high-resolution (vertical and temporal) profiling of the atmosphere over the Mace Head Atmospheric Research Station using active and passive ground-based remote sensing techniques. Cloud radar, ceilometer, microwave radiometer and wind lidar were used to obtain profiles of cloud properties, aerosol concentration, temperature, humidity and wind characteristics (speed, direction, shear, turbulence). In addition, the expansive database of past measurements was exploited to study cases of extreme air pollution (Chapter 2), to better understand cloud processes (Chapter 3) and to investigate coastal wind profiles (Chapter 4).

With a robust boundary detection algorithm, the discrimination of different aerosol layers along the vertical profiles is possible (section 2.2), and with the newly developed approach for aerosol quantification, apportionment of aerosol load per layer can be done (section 2.3). Combining those ceilometer-based products facilitated the study of extreme air pollution (section 2.4) and showed that aerosol load aloft can be decoupled from aerosol concentrations measured at the ground level. However, high aerosol concentration in the free troposphere cannot be neglected, as whatever pollution is suspended will eventually reach the ground, affecting visibility and people's health.

With a combination of three remote sensing instruments, an improved view of microphysical cloud properties was achieved (section 3.1). To gain further insight into aerosol–cloud interactions and their impact on radiative properties and the Earth's energy budget, a cloud parcel model was set up and validated against ground-based *in situ* observations, with satisfying results (section 3.1). In a next step, the model results will be compared with remote sensing products (CDNC,  $r_{\text{eff}}$ , LWC). However, case selection

proved challenging on account of restrictions of the two approaches (modelling and remote sensing).

Observing wind profiles over Mace Head for 2 years using a wind lidar, characteristics show higher wind speeds in winter months and the lowest wind speed in summer. Generally, wind direction was from the west-south-west and the prevailing wind direction was between 180° and 300°, with air arriving from that sector 55% of the time, confirming previous findings of 10-m wind characteristics (section 4.2). The profiling ability of the wind lidar enabled the observation of changes in wind speed and direction along the vertical, including wind shear, turbulence and LLJs. Such wind speed maxima along the vertical profile were mostly observed in spring and early summer, with wind direction from the east, contrary to the general prevailing wind direction.

One of the priorities of this fellowship (target number 2 in section 1.2) was to provide near real-time observations of atmospheric parameters and processes automatically and continuously. The remote sensing section of the Mace Head data display website<sup>2</sup> and all its linked sub-pages were updated hourly to provide the following:

- qualitative profiles of aerosol load from the ceilometer;<sup>3</sup>
- in-cloud profiles of cloud radar reflectivity;<sup>4</sup>
- aerosol–cloud–rain mask from combining ceilometer and cloud radar data;<sup>5</sup>
- profiles of temperature and humidity from the microwave radiometer;<sup>6</sup>
- profiles of vertical wind speed, horizontal wind speed and direction, wind shear (directional shear and speed shear), EDR and LLJ detection from Doppler lidar;<sup>7</sup>

---

2 <http://macehead.nuigalway.ie/rt/all> (accessed March 2019).

3 [http://macehead.nuigalway.ie/rt/volcano/pics/RCSignal\\_latest.png](http://macehead.nuigalway.ie/rt/volcano/pics/RCSignal_latest.png) (accessed March 2019).

4 [http://macehead.nuigalway.ie/rt/volcano/pics/Z\\_latest.png](http://macehead.nuigalway.ie/rt/volcano/pics/Z_latest.png) (accessed March 2019).

5 <http://macehead.nuigalway.ie/rt/feature> (accessed March 2019).

6 <http://macehead.nuigalway.ie/rt/hatpro.html> (accessed March 2019).

7 [http://macehead.nuigalway.ie/rt/lidar\\_63.html](http://macehead.nuigalway.ie/rt/lidar_63.html) (accessed March 2019).

- cloud microphysical products from SYRSOC<sup>8</sup> (only for certain cloud types, not publicly linked);
- comparison of WRF and lidar wind profiles<sup>9</sup> (not publicly linked);
- comparison of WRF and lidar LLJs<sup>10</sup> (not publicly linked).

## 5.1 Conclusions

The power of remote sensing lies in its ability to automatically and continuously characterise parts of the atmosphere that can be far away from the sensor, e.g. at high altitudes from the ground in the case of this study. In addition, its methods are non-intrusive, leaving the studied medium as it is, without altering its properties. Thus, remote sensing offers information that cannot be provided by ground-based *in situ* measurements. To understand what is measured at the ground level, a supplementary observation of higher altitudes is necessary, as demonstrated in the events of extreme air pollution discussed in section 2.4. In these cases, vertical profiles of aerosol load from the ceilometer contributed to answer the following questions:

- Where did the aerosol come from?
- Which type of aerosol was it?
- How long did the extreme event persist aloft and alter the amount of incoming solar radiation?
- Will there be more aerosol settling to the ground level near the ceilometer location or downwind from it?

Routine *in situ* observations of clouds are rare and commonly available only in fog or at high-altitude stations. Therefore, cloud remote sensing is necessary to solve the following questions:

- Where is the cloud base and what is the CTH?
- What are the cloud's radiative properties (optical thickness, cloud top albedo) and impact on global warming?
- How do clouds form and dissolve?
- How accurately are current cloud models representing true cloud profiles?

Wind is a common standard variable recorded at a dense network of meteorological stations worldwide. Generally, it is measured at 10 m above ground by meteorological services and fed into global forecast models. Wind profiles from remote sensing can additionally answer the following questions:

- What are the large-scale flow patterns, unaffected by local orographic features?
- How severe is vertical wind shear (direction and speed)? Is it safe to fly an aircraft or operate wind turbines?
- What is the available wind energy at the turbine height?
- Are there LLJs?

These questions cannot be answered by *in situ* observations alone. It is the combination of *in situ* and remote sensing observations, in addition to atmospheric models, that will yield the best characterisation of the state of the atmosphere at any given time.

## 5.2 Recommendations

Remote sensing at Mace Head was crucial for providing the main or auxiliary information for a number of research studies in the past few years (Dall'Osto *et al.*, 2010; Martucci *et al.*, 2010, 2012; Martucci and O'Dowd, 2011; Ovadnevaite *et al.*, 2012; Preißler *et al.*, 2016, 2019; Grigas, 2017; Sanchez *et al.*, 2017; Calmer *et al.*, 2018; Lin *et al.*, 2018). The possibilities of such studies arise from the continuous and automatic operation of these instruments for uninterrupted monitoring of the atmosphere. In addition, data are sent to European-scale networks (Cloudnet,<sup>11</sup> E-Profile<sup>12</sup>) for joint processing and large-scale studies (Illingworth *et al.*, 2007, 2015; Bühl *et al.*, 2016; Haefelin *et al.*, 2016; Lohmann *et al.*, 2018). The existence of such networks underlines the importance of ground-based remote sensing of the atmosphere at a continental scale. Remote sensing at Mace Head provides a large part of the national contribution to those pan-European networks.

8 <http://macehead.nuigalway.ie/rt/syrsoc.html> (accessed March 2019).

9 [http://macehead.nuigalway.ie/rt/wrf\\_lidar.html](http://macehead.nuigalway.ie/rt/wrf_lidar.html) (accessed March 2019).

10 [http://macehead.nuigalway.ie/rt/wrf\\_llj.html](http://macehead.nuigalway.ie/rt/wrf_llj.html) (accessed March 2019).

11 <http://devcloudnet.fmi.fi/> (accessed March 2019).

12 <https://www.eumetnet.eu/activities/observations-programme/current-activities/e-profile/> (accessed March 2019).

For a comprehensive view of the atmosphere over the Irish west coast and subsequently a better understanding and forecast of atmospheric processes such as storms, extreme pollution events and the effects of climate change, remote sensing at Mace Head will be invaluable. Continuous operation is crucial to study the complexity of coastal atmospheric processes. Furthermore, automatic processing is necessary to handle the large number of data and distil essential information from them.

Based on these considerations, continuation of remote sensing at Mace Head is highly recommended

as a supplement to the vast instrumentation (standard meteorology, *in situ* aerosol characterisation, monitoring of trace gases) existing there. The Met Éireann station Valentia in County Kerry operates a ceilometer, microwave radiometer and wind lidar and is a good example of remote sensing efforts in addition to the Mace Head Atmospheric Research Station. To extend coverage over Ireland, more remote sensing nodes should be established, preferably at existing atmospheric observatories, such as Malin Head, County Donegal, or Carnsore Point, County Wexford.

# References

- Baars, H., Kanitz, T., Engelmann, R., Althausen, D., Heese, B., Komppula, M., *et al.*, 2016. An overview of the first decade of PollyNET: an emerging network of automated Raman-polarization lidars for continuous aerosol profiling. *Atmospheric Chemistry and Physics* 16: 5111–5137. <https://doi.org/10.5194/acp-16-5111-2016>
- Bühl, J., Engelmann, R., Ansmann, A. and Seifert, P., 2016. Measuring the efficiency of ice formation in mixed-phase clouds over Europe with Cloudnet. EGU General Assembly, 17–22 April, Vienna, Austria, ID EPSC2016-4049.
- Calmer, R., Roberts, G.C., Preissler, J., Sanchez, K.J., Derrien, S. and O'Dowd, C., 2018. Vertical wind velocity measurements using a five-hole probe with remotely piloted aircraft to study aerosol–cloud interactions. *Atmospheric Measurement Techniques* 11: 2583–2599. <https://doi.org/10.5194/amt-11-2583-2018>
- Dall'Osto, M., Ceburnis, D., Martucci, G., Bialek, J., Dupuy, R., Jennings, S.G., *et al.*, 2010. Aerosol properties associated with air masses arriving into the North East Atlantic during the 2008 Mace Head EUCAARI intensive observing period: an overview. *Atmospheric Chemistry and Physics* 10: 8413–8435. <https://doi.org/10.5194/acp-10-8413-2010>
- Delanoë, J., Protat, A., Vinson, J.P., Brett, W., Caudoux, C., Bertrand, F., *et al.*, 2016. BASTA: a 95-GHz FMCW Doppler radar for cloud and fog studies. *Journal of Atmospheric and Ocean Technology* 33: 1023–1038. <https://doi.org/10.1175/JTECH-D-15-0104.1>
- Dupont, J.-C., Haeffelin, M., Wærsted, E., Delanoë, J., Renard, J.B., Preissler, J. and O'Dowd, C., 2018. Evaluation of fog and low stratus cloud microphysical properties derived from in situ sensor, cloud radar and SYRSOC algorithm. *Atmosphere* 9: 169. <https://doi.org/10.3390/atmos9050169>
- EC (European Commission), 2015. *Copernicus Brochure*. Publications Office of the European Union, Luxembourg.
- Ferek, R.J., Garrett, T., Hobbs, P.V., Strader, S., Johnson, D., Taylor, J.P., *et al.*, 2000. Drizzle suppression in ship tracks. *Journal of the Atmospheric Sciences* 57: 2707–2728. [https://doi.org/10.1175/1520-0469\(2000\)057<2707:DSIST>2.0.CO;2](https://doi.org/10.1175/1520-0469(2000)057<2707:DSIST>2.0.CO;2)
- Fossum, K.N., Ovadnevaite, J., Ceburnis, D., Dall'Osto, M., Marullo, S., Bellacicco, M., *et al.*, 2018. Summertime primary and secondary contributions to southern ocean cloud condensation nuclei. *Science Reports* 8: 13844. <https://doi.org/10.1038/s41598-018-32047-4>
- Grigas, T., 2017. Remote sensing and in-situ characterisation of atmospheric aerosol pollution. PhD Thesis. National University of Ireland Galway, Ireland. Available online: <https://aran.library.nuigalway.ie/handle/10379/6497> (accessed March 2019).
- Groß, S., Freudenthaler, V., Wirth, M. and Weinzierl, B., 2014. Towards an aerosol classification scheme for future EarthCARE lidar observations and implications for research needs. *Atmospheric Science Letters* 16: 77–82. <https://doi.org/10.1002/asl2.524>
- Haeffelin, M., Crewell, S., Illingworth, A.J., Pappalardo, G., Russchenberg, H., Chiriaco, M., Ebell, K., Hogan, R.J. and Madonna, F., 2016. Parallel developments and formal collaboration between European atmospheric profiling observatories and the US. *AMS Meteorological Monographs* 57: chapter 29. <https://doi.org/10.1175/AMSMONOGRAPHS-D-15-0045.1>
- Hervo, M., Quennehen, B., Kristiansen, N.I., Boulon, J., Stohl, A., Fréville, P., *et al.*, 2012. Physical and optical properties of 2010 Eyjafjallajökull volcanic eruption aerosol: ground-based, lidar and airborne measurements in France. *Atmospheric Chemistry and Physics* 12: 1721–1736. <https://doi.org/10.5194/acp-12-1721-2012>
- Hirth, L. and Müller, S., 2016. System-friendly wind power: how advanced wind turbine design can increase the economic value of electricity generated through wind power. *Energy Economics* 56: 51–63. <https://doi.org/10.1016/j.eneco.2016.02.016>
- ICAO (International Civil Aviation Organization), 2018. *Safety Report*. ICAO. Available online: [https://www.icao.int/safety/Documents/ICAO\\_SR\\_2018\\_30082018.pdf](https://www.icao.int/safety/Documents/ICAO_SR_2018_30082018.pdf) (accessed March 2019).
- Illingworth, A.J., Hogan, R.J., O'Connor, E.J., Bouniol, D., Brooks, M.E., Delanoë, J., *et al.*, 2007. Cloudnet: continuous evaluation of cloud profiles in seven operational models using ground-based observations. *Bulletin of the American Meteorological Society* 88: 883–898. <https://doi.org/10.1175/BAMS-88-6-883>

- Illingworth, A.J., Cimini, D., Gaffard, C., Haeffelin, M., Lehmann, V., Löhnert, U., O'Connor, E.J. and Ruffieux, D., 2015. Exploiting existing ground-based remote sensing networks to improve high-resolution weather forecasts. *Bulletin of the American Meteorological Society* 96: 2107–2125. <https://doi.org/10.1175/BAMS-D-13-00283.1>
- Jennings, S.G., Kleefeld, C., O'Dowd, C.D., Junker, C., Spain, T.G., O'Brien, P., Roddy, A.F. and O'Connor, T.C., 2003. Mace Head Atmospheric Research Station – characterization of aerosol radiative parameters. *Boreal Environment Research* 8: 303314.
- Kumer, V.-M., Reuder, J., Dorninger, M., Zauner, R. and Grubisic, V., 2016. Turbulent kinetic energy estimates from profiling wind lidar measurements and their potential for wind energy applications. *Renewable Energy* 99: 898–910. <https://doi.org/10.1016/j.renene.2016.07.014>
- Li, Z., Guo, J., Ding, A., Liao, H., Liu, J., Sun, Y., Wang, T., Xue, H., Zhang, H. and Zhu, B., 2017. Aerosol and boundary–layer interactions and impact on air quality. *National Science Review* 4: 810–833. <https://doi.org/10.1093/nsr/nwx117>
- Lin, C., Huang, R.-J., Ceburnis, D., Buckley, P., Preissler, J., Wenger, J., Rinaldi, M., Facchini, M.C., O'Dowd, C. and Ovadnevaite, J., 2018. Extreme air pollution from residential solid fuel burning. *Nature Sustainability* 1: 512–517. <https://doi.org/10.1038/s41893-018-0125-x>
- Lohmann, U. and Feichter, J., 2005. Global indirect aerosol effects: a review. *Atmospheric Chemistry and Physics* 5: 715–737. <https://doi.org/10.5194/acp-5-715-2005>
- Lohmann, U., Burkert, M., Ansmann, A., Facchini, C., Kanakidou, M., Stier, P., et al., 2018. *BACCHUS: Impact of Biogenic versus Anthropogenic Emissions on Clouds and Climate: Towards a Holistic Understanding. Final Summary for Policy Makers*. Available online: [https://www.bacchus-env.eu/public/Deliverables/D5.8\\_FinalSummaryPolicyMakers\\_BACCHUS\\_final.pdf](https://www.bacchus-env.eu/public/Deliverables/D5.8_FinalSummaryPolicyMakers_BACCHUS_final.pdf) (accessed March 2019).
- Manninen, A.J., O'Connor, E.J., Vakkari, V. and Petäjä, T., 2016. A generalised background correction algorithm for a Halo Doppler lidar and its application to data from Finland. *Atmospheric Measurement Techniques* 9: 817–827. <https://doi.org/10.5194/amt-9-817-2016>
- Martucci, G. and O'Dowd, C.D., 2011. Ground-based retrieval of continental and marine warm cloud microphysics. *Atmospheric Measurement Techniques* 4: 2749–2765. <https://doi.org/10.5194/amt-4-2749-2011>
- Martucci, G., Milroy, C. and O'Dowd, C.D., 2010. Detection of cloud base height using Jenoptik CHM15k and Vaisala CL31 ceilometers. *Journal of Atmospheric and Oceanic Technology* 27: 305–318. <https://doi.org/10.1175/2009JTECHA1326.1>
- Martucci, G., Ovadnevaite, J., Ceburnis, D., Berresheim, H., Varghese, S., Martin, D., Flanagan, R. and O'Dowd, C.D., 2012. Impact of volcanic ash plume aerosol on cloud microphysics. *Atmospheric Environment* 48: 205–218. <https://doi.org/10.1016/j.atmosenv.2011.12.033>
- Miles, N.L., Verlinde, J. and Clothiaux, E.E., 2000. Cloud droplet size distributions in low-level stratiform clouds. *Journal of the Atmospheric Sciences* 57: 295–311. [https://doi.org/10.1175/1520-0469\(2000\)057<0295:CDSDIL>2.0.CO;2](https://doi.org/10.1175/1520-0469(2000)057<0295:CDSDIL>2.0.CO;2)
- Müller, D., Ansmann, A., Mattis, I., Tesche, M., Wandinger, U., Althausen, D. and Pisani, G., 2007. Aerosol-type-dependent lidar ratios observed with Raman lidar. *Journal of Geophysical Research Atmospheres* 112: D16202. <https://doi.org/10.1029/2006JD008292>
- O'Dowd, C., Lowe, J.A., Clegg, N., Smith, M.H. and Clegg, S.L., 2000. Modeling heterogeneous sulphate production in maritime stratiform clouds. *Journal of Geophysical Research Atmospheres* 105: 7143–7160. <https://doi.org/10.1029/1999JD900915>
- Ovadnevaite, J., Ceburnis, D., Canagaratna, M., Berresheim, H., Bialek, J., Martucci, G., Worsnop, D.R. and O'Dowd, C., 2012. On the effect of wind speed on submicron sea salt mass concentrations and source fluxes. *Journal of Geophysical Research Atmospheres* 117: D16201. <https://doi.org/10.1029/2011JD017379>
- Päschke, E., Leinweber, R. and Lehmann, V., 2015. An assessment of the performance of a 1.5µm Doppler lidar for operational vertical wind profiling based on a 1-year trial. *Atmospheric Measurement Techniques* 8: 2251–2266. <https://doi.org/10.5194/amt-8-2251-2015>
- Preißler, J., Martucci, G., Saponaro, G., Ovadnevaite, J., Vaishya, A., Kolmonen, P., Ceburnis, D., Sogacheva, L., de Leeuw, G. and O'Dowd, C., 2016. Six years of surface remote sensing of stratiform warm clouds in marine and continental air over Mace Head, Ireland. *Journal of Geophysical Research Atmospheres* 121: 14538–14557. <https://doi.org/10.1002/2016JD025360>
- Preißler, J., Martucci, G. and O'Dowd, C.D., 2019. *Ground-based Remote-sensing Synergy for Cloud Properties and Aerosol–Cloud Interactions*. Environmental Protection Agency, Johnstown Castle, Ireland.

- Roebeling, R.A., Feijt, A.J. and Stammes, P., 2006. Cloud property retrievals for climate monitoring: implications of differences between Spinning Enhanced Visible and Infrared Imager (SEVIRI) on METEOSAT-8 and Advanced Very High Resolution Radiometer (AVHRR) on NOAA-17. *Journal of Geophysical Research Atmospheres* 111: D20210. <https://doi.org/10.1029/2005JD006990>
- Rosenfeld, D., Lohmann, U., Raga, G.B., O'Dowd, C.D., Kulmala, M., Fuzzi, S., Reissell, A. and Andreae, M.O., 2008. Flood or drought: how do aerosols affect precipitation?. *Science* 321: 1309–1313. <https://doi.org/10.1126/science.1160606>
- Sanchez, K.J., Roberts, G.C., Calmer, R., Nicoll, K., Hashimshoni, E., Rosenfeld, D., Ovadnevaite, J., Preissler, J., Ceburnis, D., O'Dowd, C. and Russell, L.M., 2017. Top-down and bottom-up aerosol–cloud closure: towards understanding sources of uncertainty in deriving cloud shortwave radiative flux. *Atmospheric Chemistry and Physics* 17: 9797–9814. <https://doi.org/10.5194/acp-17-9797-2017>
- Sekelsky, S.M., 2002. Near-field reflectivity and antenna boresight gain corrections for millimeter-wave atmospheric radars. *Journal of Atmospheric and Oceanic Technology* 19: 468–477. [https://doi.org/10.1175/1520-0426\(2002\)019<0468:NFRAAB>2.0.CO;2](https://doi.org/10.1175/1520-0426(2002)019<0468:NFRAAB>2.0.CO;2)
- Sharman, R. and Lane, T. (eds), 2016. *Aviation Turbulence: Processes, Detection, Prediction*. Springer International Publishing, Cham, Switzerland.
- Shen, X., Zhu, X. and Du, Z., 2011. Wind turbine aerodynamics and loads control in wind shear flow. *Energy* 36: 1424–1434. <https://doi.org/10.1016/j.energy.2011.01.028>
- Stocker, T.F., Qin, D., Plattner, G.-K., Tignor, M., Allen, S.K., Boschung, J., Nauels, A., Xia, Y., Bex, V. and Midgley, P.M. (eds), 2013. *Climate Change 2013: The Physical Science Basis*. Contribution of Working Group I to the Fifth Assessment Report of the Intergovernmental Panel on Climate Change. Cambridge University Press, Cambridge, UK.
- Tie, X., Huang, R.-J., Cao, J., Zhang, Q., Cheng, Y., Su, H., *et al.*, 2017. Severe pollution in China amplified by atmospheric moisture. *Scientific Reports* 7: 15760. <https://doi.org/10.1038/s41598-017-15909-1>
- Tuononen, M., O'Connor, E.J., Sinclair, V.A. and Vakkari, V., 2017. Low-level jets over Utö, Finland, based on Doppler lidar observations. *Journal of Applied Meteorology and Climatology* 56: 2577–2594. <https://doi.org/10.1175/JAMC-D-16-0411.1>
- Twomey, S., 1977. The influence of pollution on shortwave albedo of clouds. *Journal of the Atmospheric Sciences* 34: 1149–1152. [https://doi.org/10.1175/1520-0469\(1977\)034<1149:TIOPOT>2.0.CO;2](https://doi.org/10.1175/1520-0469(1977)034<1149:TIOPOT>2.0.CO;2)
- Wagner, R., Courtney, M., Gottschall, J. and Lindelöw-Marsden, P., 2011. Accounting for the speed shear in wind turbine power performance measurement. *Wind Energy* 14: 993–1004. <https://doi.org/10.1002/we.509>
- Yang, S., Petersen, G.N., von Löwis, S., Preißler, J. and Finger, D.C., 2019. Using Doppler lidar systems to detect atmospheric turbulence in Iceland. *Atmospheric Measurement Techniques Discussion*. <https://doi.org/10.5194/amt-2019-3>

# Abbreviations

|                  |  |
|------------------|--|
| <b>ABL</b>       | Atmospheric boundary layer   |
| <b>ACTRIS</b>    | Aerosol, Clouds and Trace gases Research Infrastructure  |
| <b>agl</b>       | Above ground level   |
| <b>BASTA</b>     | Bistatic Radar System for Atmospheric Studies  |
| <b>BC</b>        | Black carbon   |
| <b>CAMS</b>      | Copernicus Atmosphere Monitoring Service   |
| <b>CCN</b>       | Cloud condensation nuclei  |
| <b>CDNC</b>      | Cloud droplet number concentration   |
| <b>Cix</b>       | Confidence index   |
| <b>CNR</b>       | Carrier-to-noise ratio   |
| <b>COST</b>      | European Cooperation in Science and Technology   |
| <b>COT</b>       | Cloud optical thickness  |
| <b>CP</b>        | Continental polar (air mass)   |
| <b>CTH</b>       | Cloud top height   |
| <b>eBC</b>       | Equivalent black carbon  |
| <b>EDR</b>       | Eddy dissipation rate  |
| <b>EUMETNET</b>  | Network of European National Meteorological Services   |
| <b>FMI</b>       | Finnish Meteorological Institute   |
| <b>HATPRO</b>    | Humidity and Temperature Profiler  |
| <b>IBS</b>       | Integrated backscatter   |
| <b>KNMI</b>      | Royal Netherlands Meteorological Institute (Koninklijk Nederlands Meteorologisch Instituut)            |
| <b>LLJ</b>       | Low-level jet  |
| <b>LOAC</b>      | Light optical aerosol counter  |
| <b>LOS</b>       | Line of sight  |
| <b>LR</b>        | Lidar ratio  |
| <b>LWC</b>       | Liquid water content   |
| <b>LWP</b>       | Liquid water path  |
| <b>MER</b>       | Mass-to-extinction ratio   |
| <b>MP</b>        | Marine polar (air mass)  |
| <b>MSG</b>       | Meteosat Second Generation   |
| <b>NUIG</b>      | National University of Ireland, Galway   |
| $r_{\text{eff}}$ | Effective cloud droplet radius   |
| <b>RL</b>        | Residual layer   |
| <b>SEVIRI</b>    | Spinning Enhanced Visible and Infrared Imager  |
| <b>SIRTA</b>     | Site Instrumental de Recherche par Télédétection Atmosphérique (research station in Palaiseau, France) |
| <b>SYRSOC</b>    | Synergistic Remote Sensing Of Clouds   |
| <b>UTC</b>       | Coordinated Universal Time   |
| <b>VAD</b>       | Velocity azimuth display   |
| <b>WRF</b>       | Weather Research Forecast  |



## AN GHNÍOMHAIREACTH UM CHAOMHNÚ COMHSHAOIL

Tá an Gníomhaireacht um Chaomhnú Comhshaoil (GCC) freagrach as an gcomhshaoil a chaomhnú agus a fheabhsú mar shócmhainn luachmhar do mhuintir na hÉireann. Táimid tiomanta do dhaoine agus don chomhshaoil a chosaint ó éifeachtaí díobhálacha na radaíochta agus an truaillithe.

## Is féidir obair na Gníomhaireachta a roinnt ina trí phríomhréimse:

**Rialú:** Déanaimid córais éifeachtacha rialaithe agus comhlionta comhshaoil a chur i bhfeidhm chun torthaí maithe comhshaoil a sholáthar agus chun díriú orthu siúd nach gcloíonn leis na córais sin.

**Eolas:** Soláthraimid sonraí, faisnéis agus measúnú comhshaoil atá ar ardchaighdeán, spriocdhírthe agus tráthúil chun bonn eolais a chur faoin gcinnteoireacht ar gach leibhéal.

**Tacaíocht:** Bimid ag saothrú i gcomhar le grúpaí eile chun tacú le comhshaoil atá glan, táirgiúil agus cosanta go maith, agus le hiompar a chuirfidh le comhshaoil inbhuanaithe.

## Ár bhFreagrachtaí

### Ceadúnú

Déanaimid na gníomhaíochtaí seo a leanas a rialú ionas nach ndéanann siad dochar do shláinte an phobail ná don chomhshaoil:

- saoráidí dramhaíola (*m.sh. láithreáin líonta talún, loisceoirí, stáisiúin aistriúcháin dramhaíola*);
- gníomhaíochtaí tionsclaíocha ar scála mór (*m.sh. déantúsaíocht cógaisíochta, déantúsaíocht stroighne, stáisiúin chumhachta*);
- an diantalmhaíocht (*m.sh. muca, éanlaith*);
- úsáid shrianta agus scaoileadh rialaithe Orgánach Géinmhodhnaithe (*OGM*);
- foinsí radaíochta ianúcháin (*m.sh. trealamh x-gha agus radaiteiripe, foinsí tionsclaíocha*);
- áiseanna móra stórála peitрил;
- scardadh dramhuisece;
- gníomhaíochtaí dumpála ar farraige.

### Forfheidhmiú Náisiúnta i leith Cúrsaí Comhshaoil

- Clár náisiúnta iniúchtaí agus cigireachtaí a dhéanamh gach bliain ar shaoráidí a bhfuil ceadúnas ón nGníomhaireacht acu.
- Maoirseacht a dhéanamh ar fhreagrachtaí cosanta comhshaoil na n-údarás áitiúil.
- Caighdeán an uisce óil, arna sholáthar ag soláthraithe uisce phoiblí, a mhaoirsiú.
- Obair le húdarás áitiúla agus le gníomhaireachtaí eile chun dul i ngleic le coireanna comhshaoil trí chomhordú a dhéanamh ar líonra forfheidhmiúcháin náisiúnta, trí dhírú ar chiontóirí, agus trí mhaoirsiú a dhéanamh ar leasúchán.
- Cur i bhfeidhm rialachán ar nós na Rialachán um Dhramhthrealamh Leictreach agus Leictreonach (DTLL), um Shrian ar Shubstaintí Guaiseacha agus na Rialachán um rialú ar shubstaintí a ídionn an ciseal ózóin.
- An dlí a chur orthu siúd a bhriseann dlí an chomhshaoil agus a dhéanann dochar don chomhshaoil.

### Bainistíocht Uisce

- Monatóireacht agus tuairisciú a dhéanamh ar cháilíocht aibhneacha, lochanna, uisce idirchriosacha agus cósta na hÉireann, agus screamhuisec; leibhéal uisce agus sruthanna aibhneacha a thomhas.
- Comhordú náisiúnta agus maoirsiú a dhéanamh ar an gCreat-Treoir Uisce.
- Monatóireacht agus tuairisciú a dhéanamh ar Cháilíocht an Uisce Snámha.

## Monatóireacht, Anailís agus Tuairisciú ar an gComhshaoil

- Monatóireacht a dhéanamh ar cháilíocht an aeir agus Treoir an AE maidir le hAer Glan don Eoraip (CAFÉ) a chur chun feidhme.
- Tuairisciú neamhspleách le cabhrú le cinnteoireacht an rialtais náisiúnta agus na n-údarás áitiúil (*m.sh. tuairisciú tréimhsiúil ar staid Chomhshaoil na hÉireann agus Tuarascálacha ar Tháscairí*).

## Rialú Astaíochtaí na nGás Ceaptha Teasa in Éirinn

- Fardail agus réamh-mheastacháin na hÉireann maidir le gáis ceaptha teasa a ullmhú.
- An Treoir maidir le Trádáil Astaíochtaí a chur chun feidhme i gcomhar breis agus 100 de na táirgeoirí dé-ocsaíde carbóin is mó in Éirinn.

## Taighde agus Forbairt Comhshaoil

- Taighde comhshaoil a chistiú chun brúnna a shainathint, bonn eolais a chur faoi bheartais, agus réitigh a sholáthar i réimsí na haeráide, an uisce agus na hinbhuanaitheachta.

## Measúnacht Straitéiseach Timpeallachta

- Measúnacht a dhéanamh ar thionchar pleananna agus clár beartaithe ar an gcomhshaoil in Éirinn (*m.sh. mórfheananna forbartha*).

## Cosaint Raideolaíoch

- Monatóireacht a dhéanamh ar leibhéal radaíochta, measúnacht a dhéanamh ar nochtadh mhuintir na hÉireann don radaíocht ianúcháin.
- Cabhrú le pleananna náisiúnta a fhorbairt le haghaidh éigeandálaí ag eascairt as tairmí núicléacha.
- Monatóireacht a dhéanamh ar fhorbairtí thar lear a bhaineann le saoráidí núicléacha agus leis an tsábháilteacht raideolaíochta.
- Sainseirbhísí cosanta ar an radaíocht a sholáthar, nó maoirsiú a dhéanamh ar sholáthar na seirbhísí sin.

## Treoir, Faisnéis Inrochtana agus Oideachas

- Comhairle agus treoir a chur ar fáil d'earnáil na tionsclaíochta agus don phobal maidir le hábhair a bhaineann le caomhnú an chomhshaoil agus leis an gcosaint raideolaíoch.
- Faisnéis thráthúil ar an gcomhshaoil ar a bhfuil fáil éasca a chur ar fáil chun rannpháirtíocht an phobail a spreagadh sa chinnteoireacht i ndáil leis an gcomhshaoil (*m.sh. Timpeall an Tí, léarscáileanna radóin*).
- Comhairle a chur ar fáil don Rialtas maidir le hábhair a bhaineann leis an tsábháilteacht raideolaíoch agus le cúrsaí práinnfhreagartha.
- Plean Náisiúnta Bainistíochta Dramhaíola Guaisí a fhorbairt chun dramhaíl ghuaiseach a chosaint agus a bhainistiú.

## Múscail Feasachta agus Athrú Iompraíochta

- Feasacht chomhshaoil níos fearr a ghiniúint agus dul i bhfeidhm ar athrú iompraíochta dearfach trí thacú le gnóthais, le pobail agus le teaghlaigh a bheith níos éifeachtúla ar acmhainní.
- Tástáil le haghaidh radóin a chur chun cinn i dtithe agus in ionaid oibre, agus gníomhartha leasúcháin a spreagadh nuair is gá.

## Bainistíocht agus struchtúr na Gníomhaireachta um Chaomhnú Comhshaoil

Tá an ghníomhaíocht á bainistiú ag Bord Iáinimseartha, ar a bhfuil Ard-Stiúrthóir agus cúigear Stiúrthóirí. Déantar an obair ar fud cúig cinn d'Oifigí:

- An Oifig um Inmharthanacht Comhshaoil
- An Oifig Forfheidhmithe i leith cúrsaí Comhshaoil
- An Oifig um Fianaise is Measúnú
- Oifig um Chosaint Radaíochta agus Monatóireachta Comhshaoil
- An Oifig Cumarsáide agus Seirbhísí Corparáideacha

Tá Coiste Comhairleach ag an nGníomhaireacht le cabhrú léi. Tá dáréag comhaltáí air agus tagann siad le chéile go rialta le plé a dhéanamh ar ábhair inní agus le comhairle a chur ar an mBord.

## Remote Sensing of Aerosols, Clouds and Wind at Mace Head Atmospheric Research Station



Authors: Jana Preißler and Colin O'Dowd

### Identifying pressures

The anthropogenic impact on air quality, weather and climate, and by extension on the economy, is a present concern for scientists, policymakers and the public. In recent years, attention has also been drawn towards the hazards that volcanic eruptions pose to the economy, air quality and human health. These events, although infrequent, can have a very strong impact on the Irish public by disrupting air traffic, increasing air pollution and affecting health. This project focused on continuous high-resolution (vertical and temporal) profiling of the atmosphere over Mace Head Atmospheric Research Station using active and passive ground-based remote sensing techniques to address some of these challenges. A cloud radar, ceilometer, microwave radiometer and wind lidar were used to obtain profiles of cloud properties, aerosol concentration, temperature, humidity, and wind characteristics (speed, direction, shear, turbulence).

### Developing solutions

The transport of man-made and naturally occurring pollutants, their quantification and characterisation, and their interaction with clouds and therefore their impact on the climate can be studied with the help of active and passive remote sensing instruments. Sophisticated sensors on the ground enable highly temporally and vertically resolved observations of atmospheric components such as clouds and aerosols, as well as atmospheric parameters such as wind speed, wind direction, temperature and humidity, to be carried out. The remote sensing division of the Mace Head Atmospheric Research Station includes all of these capabilities. In addition, the large set of co-located ground-based in situ instrumentation for the measurement of aerosol properties can aid in the accurate characterisation of pollutants and forms the link from the ground to vertical profiles provided by the remote sensing instruments. The detection of transboundary transport of air pollution was addressed with the suite of remote sensing instruments at Mace Head, in combination with transport models and trajectories. These tools enable the identification of aerosol origin and thus support the characterisation of emission sources. With Mace Head's capabilities we can also detect volcanic aerosol plumes (ash particles, as well as sulfuric acid droplets). With the closest volcanic sources located in Iceland, Mace Head is a prime site for early detection of such plumes. The remote sensing data can be used to alert Ireland and Europe about volcanic aerosol advection in the case of westerly and north-westerly winds.

### Informing policy

As well as contributing to high-impact research studies in past years, remote sensing data were sent to the European-scale networks Cloudnet and E-Profile for joint processing and large-scale studies. The existence of such networks underlines the importance of ground-based remote sensing of the atmosphere on a continental scale. Remote sensing at Mace Head provides a large part of the Irish contribution to these pan-European networks. For a comprehensive view of the atmosphere over the Irish west coast and subsequently a better understanding and forecast of atmospheric processes such as storms, extreme pollution events and the effects of climate change, remote sensing at Mace Head is invaluable. Continuous operation is crucial to study the complexity of coastal atmospheric processes, and automatic processing is necessary to handle large amounts of data and distil essential information from the data.